The Near-Surface Layer of the Ocean

Alex Soloviev

All-Hands Meeting

October 2-4, 2013

Coconut Grove, FL

Content

1. Sea surface microlayer
2. Turbulence and fine structure
3. Spatial and coherent structures
4. Strong winds
5. Conclusions

Sea Surface Microlayer

The top few millimeters of the ocean surface where physical and biochemical properties are altered relative to deeper water

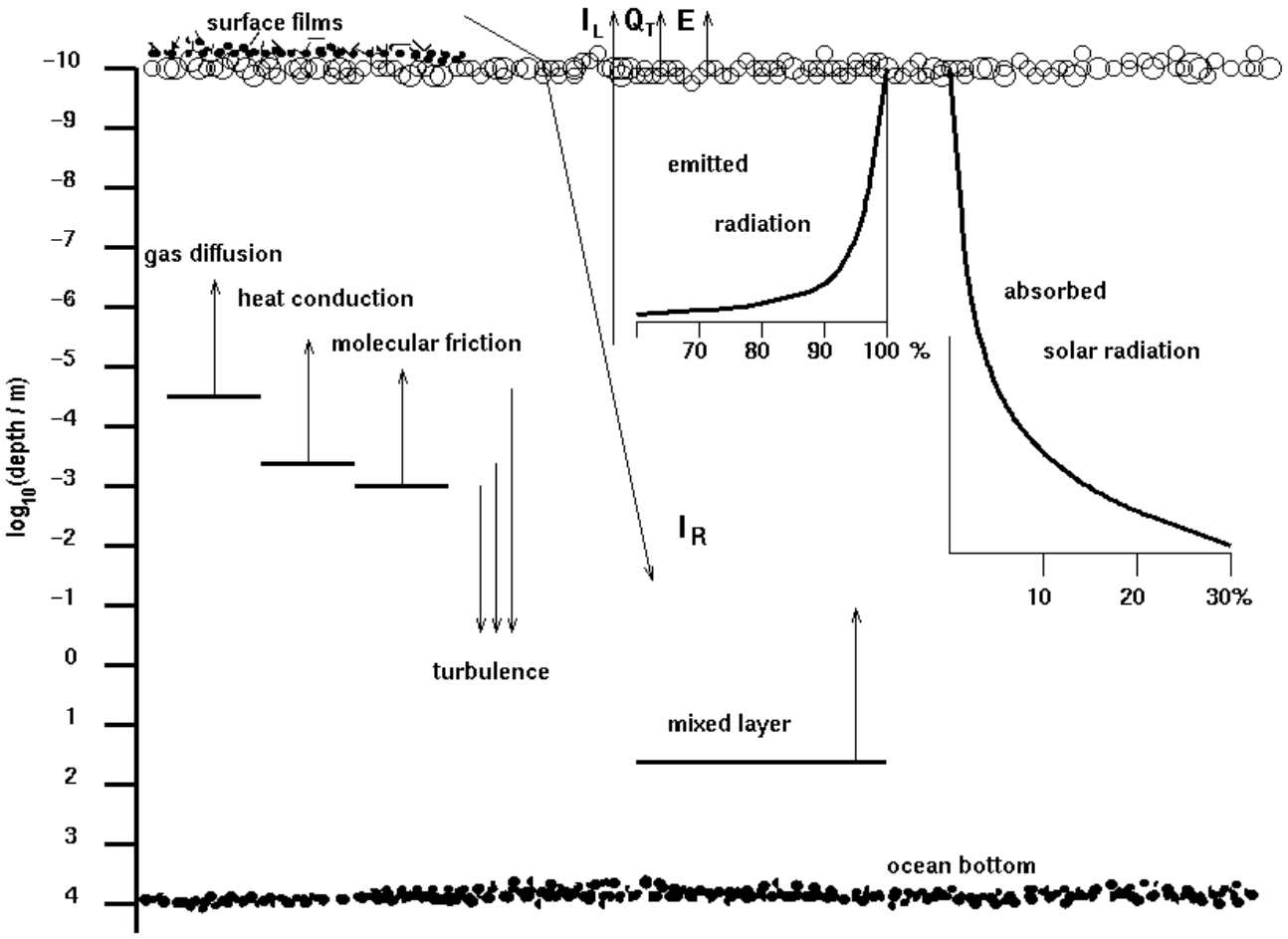

Courtesy of Peter Schluessel, EUMETSAT

Thermal Molecular Diffusion Sublayer (Cool Skin)

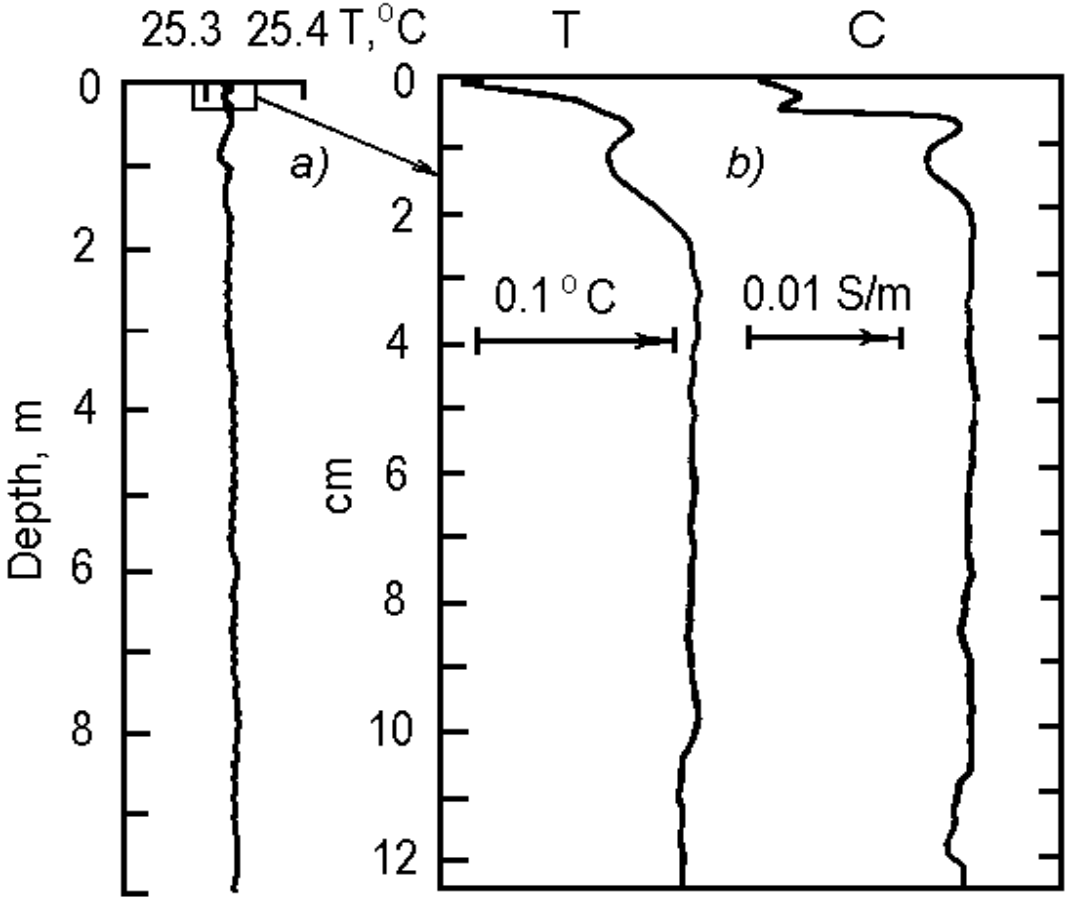

Soloviev and Vershinsky (1982)

Cool Skin on the Top of Diurnal Warm Layer

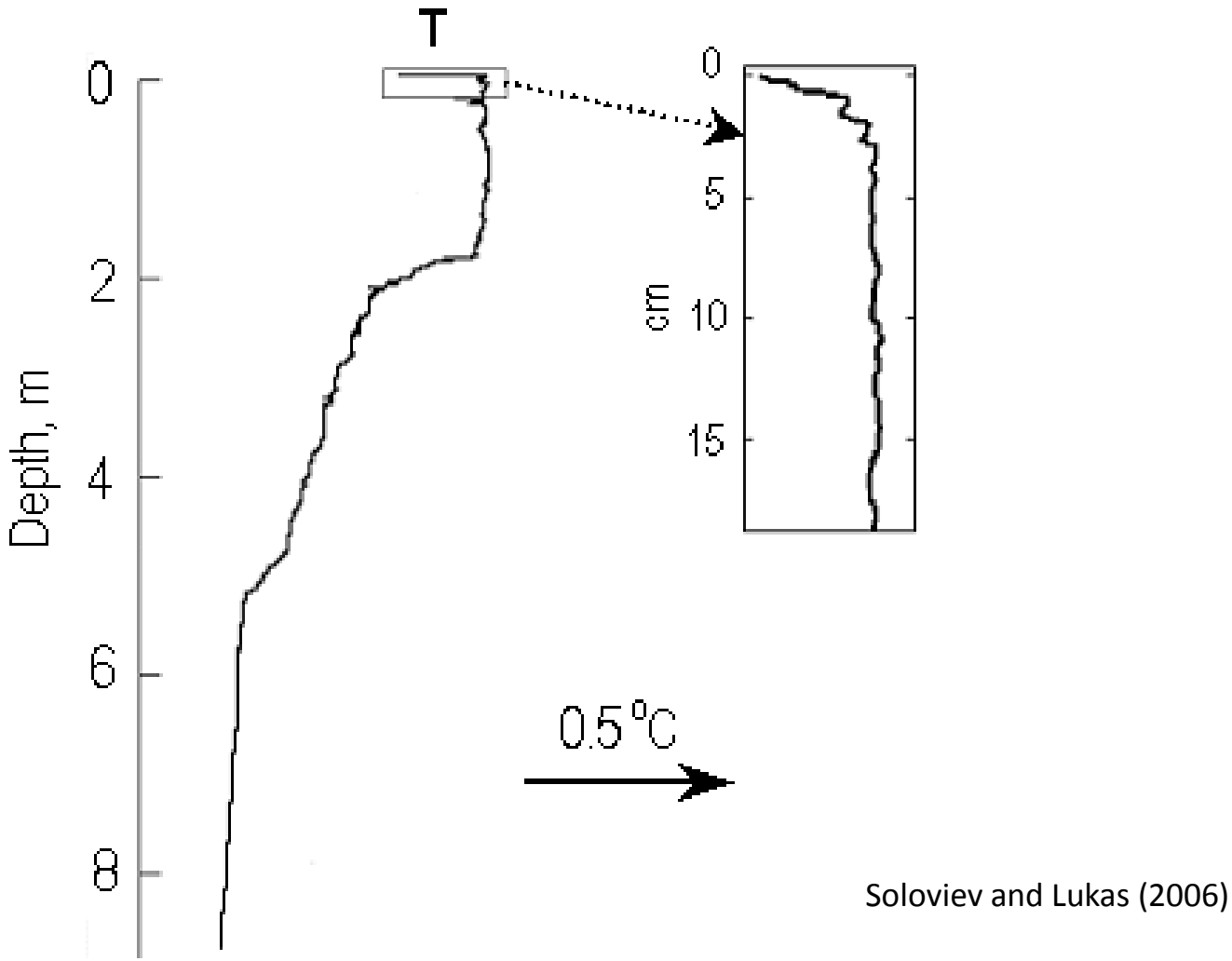

Soloviev and Lukas (2006)

Vertical profile of temperature in the upper ocean under low wind speed conditions and diurnal warming

Infrared SST and 5 m Temperature Differences

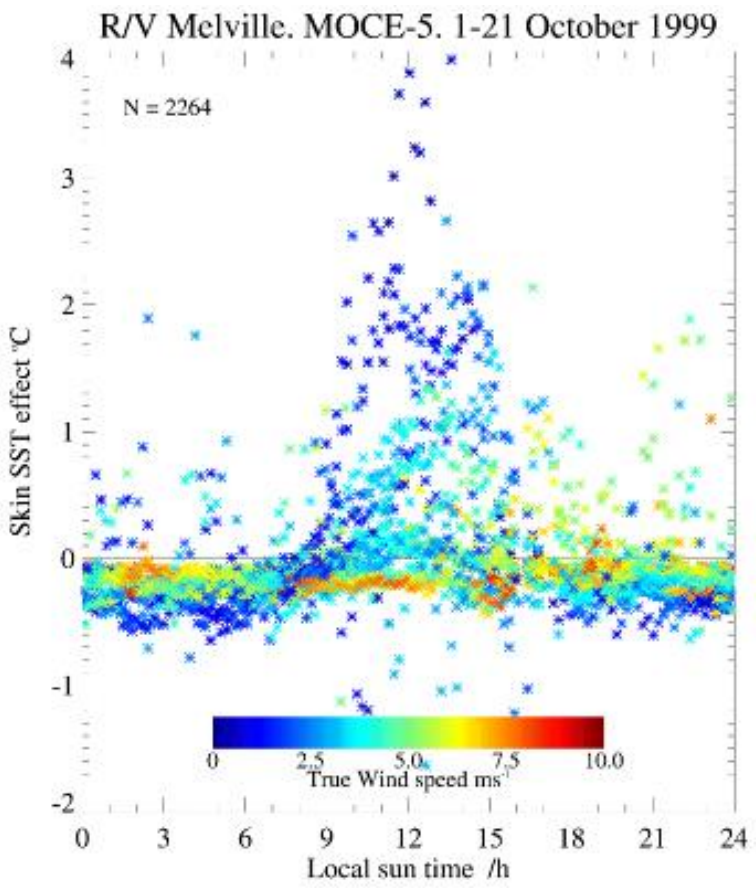

Diurnal cycle

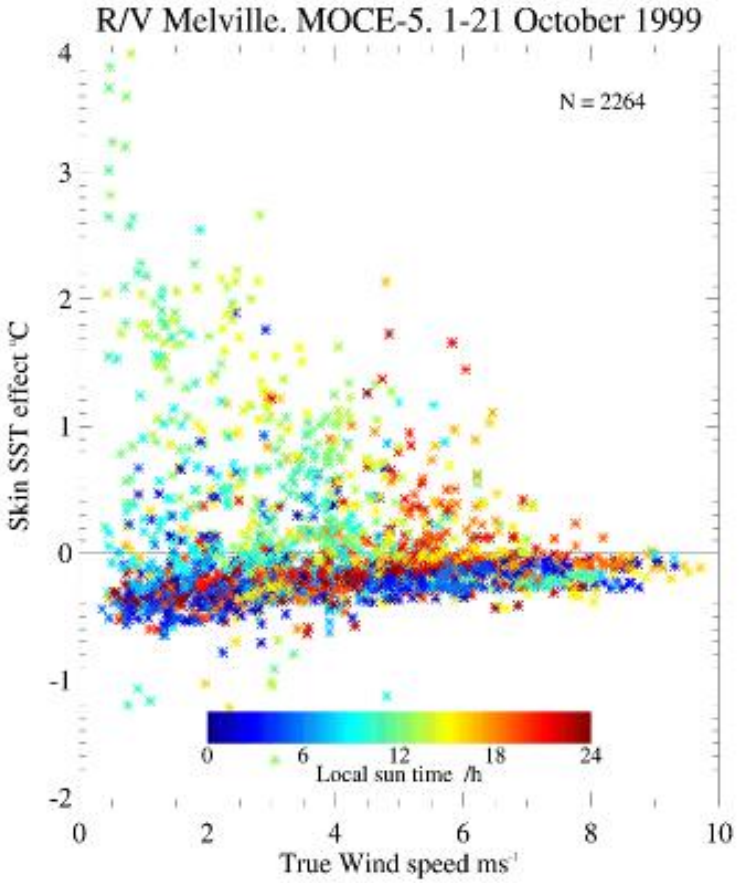

Wind speed dependence

Large temperature differences can be observed in the upper few meters of the ocean under low wind speed conditions

Minnett (2003)

Effect of Surfactants on Molecular Sublayers

Microlayer Ecosystem

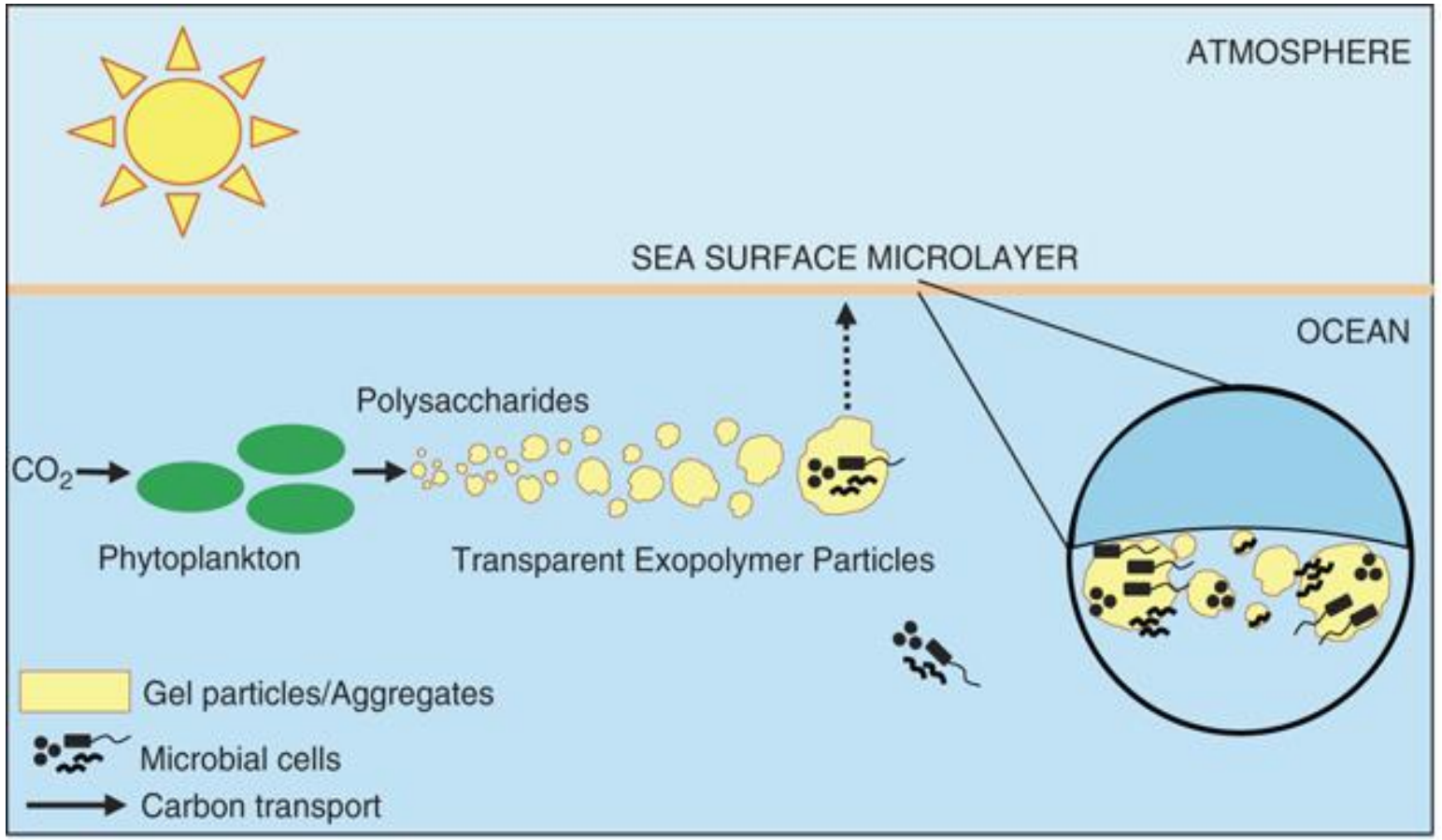

Wurl and Holmes (2008)

Chemical Structure of Slick-forming Substances (Surfactants)

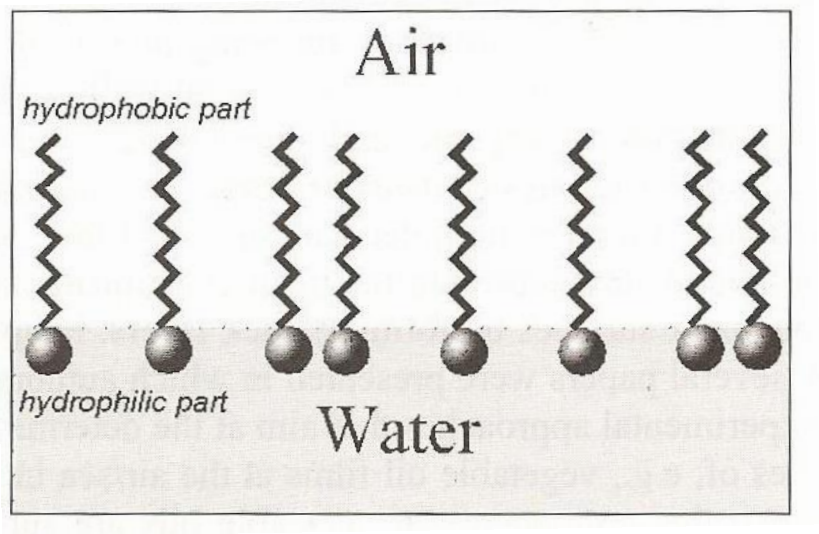

Monomolecular surface film
formed by surfactant (2.4-2.7 nm)

Huehnerfuss (2008)

Simulation of Surfactant Effects with Computational Fluid Dynamics (CFD)

Length, m	Width, m	Height, m	Δx, m	Δy, m	Δz, m	Growth Rate
0.5	0.5	0.5	0.0025	0.0025	0.001	1.1

0.5 m x 0.5 m x 0.5 m

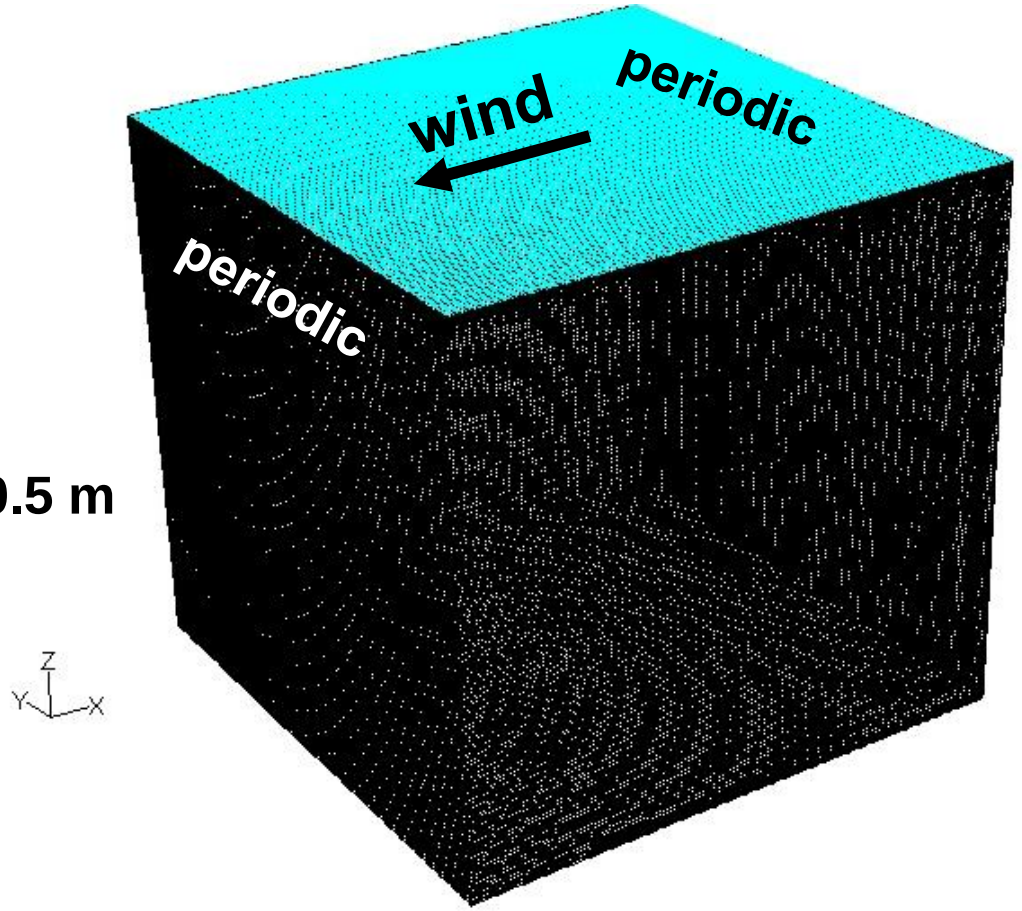

Matt et al. (2011)

Elastic Boundary Condition

Wind stress | **Surfactant Marangoni stress** | **Temperature Marangoni stress**

$$\tau_x = \tau_{wind} + \partial\sigma/\partial C \cdot \partial C/\partial x + \partial\sigma/\partial T \cdot \partial T/\partial x$$

$$\tau_y = \partial\sigma/\partial C \cdot \partial C/\partial y + \partial\sigma/\partial T \cdot \partial T/\partial y$$

σ – **surface tension**

C – **surfactant concentration**

T – **water surface temperature**

No Surfactant - Top view: U at top (z = 0 cm)

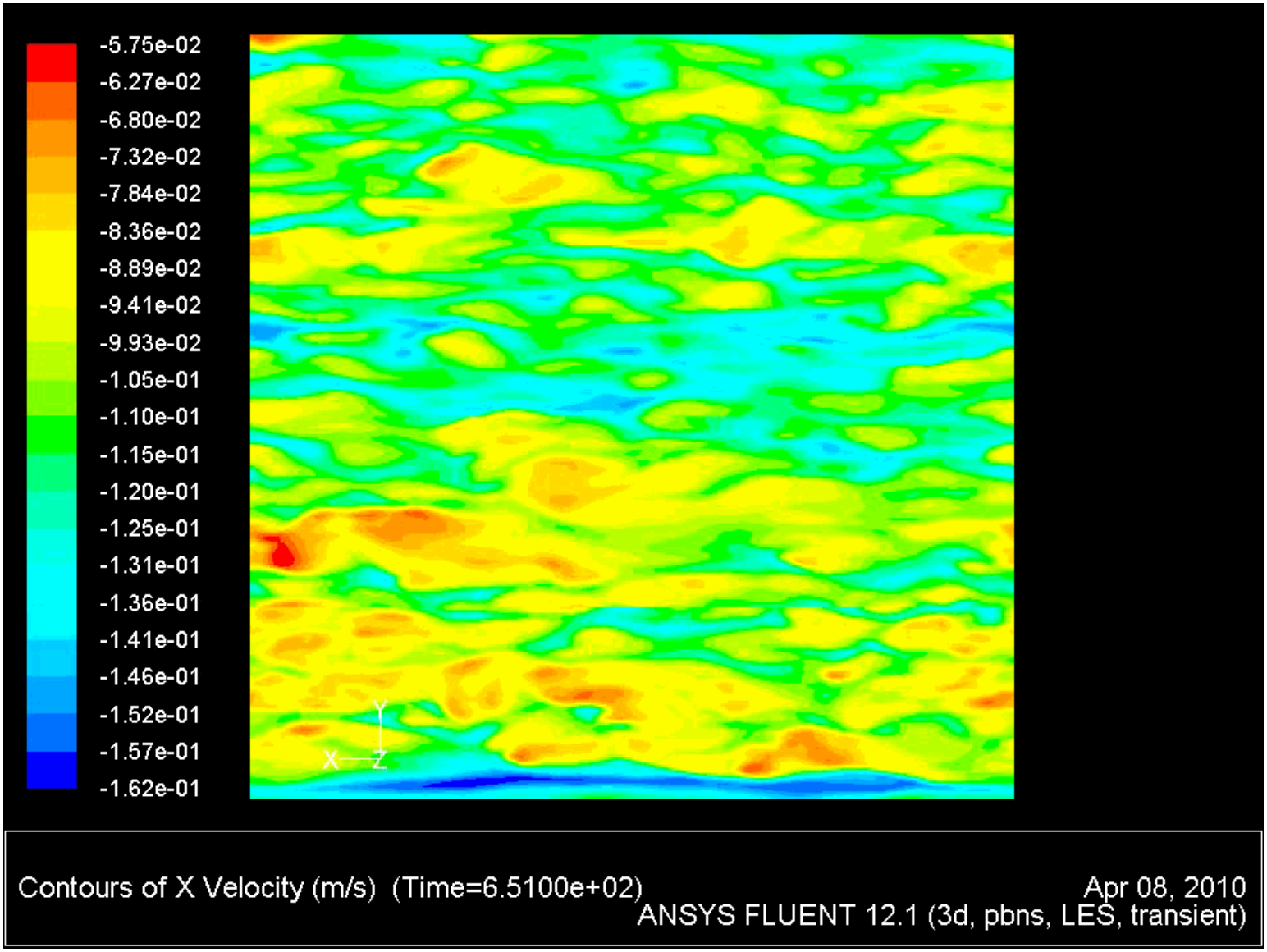

With Surfactant - Top view: U at top (z = 0 cm)

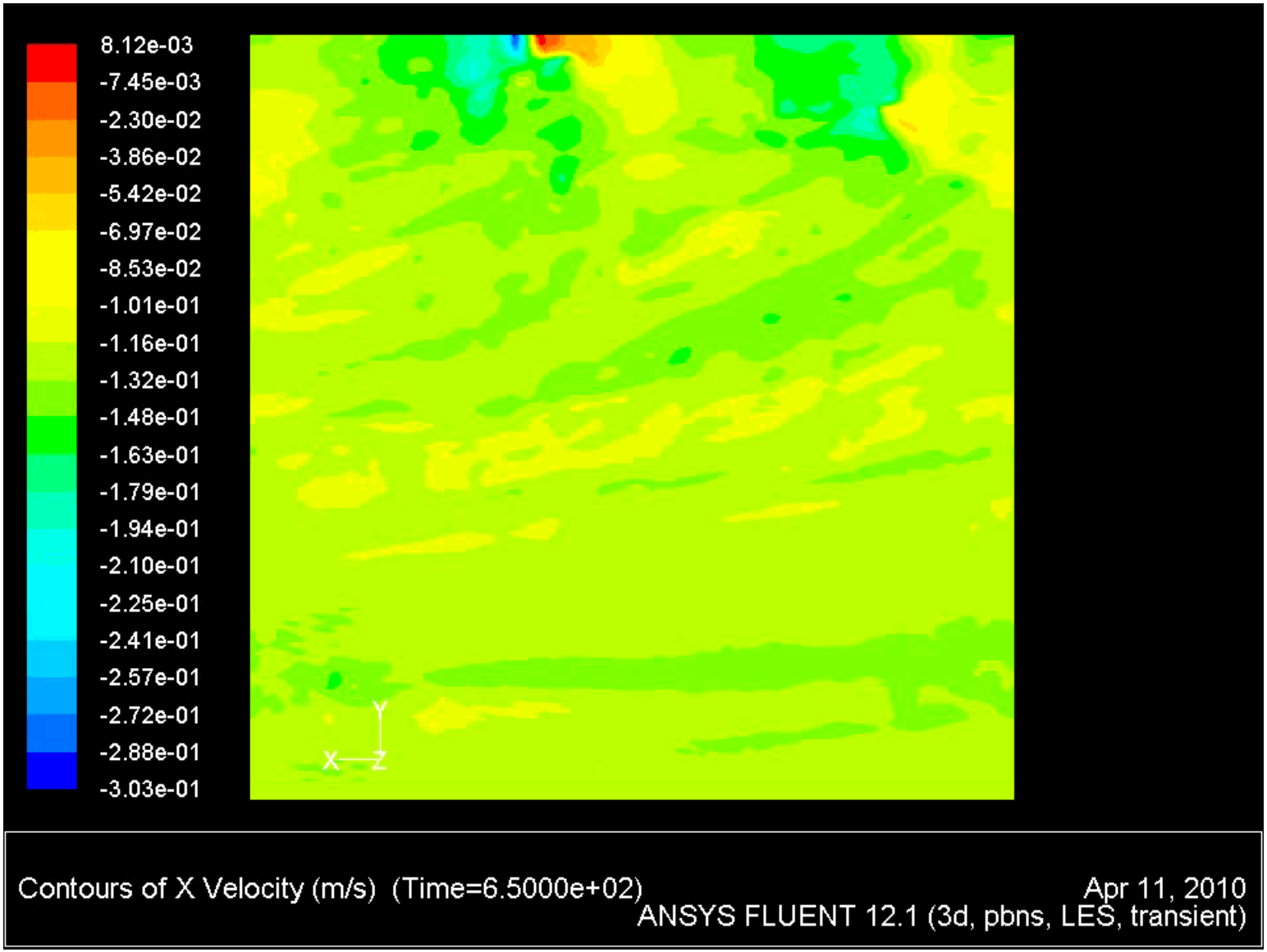

Surfactants suppress coherent streaks and turbulence in the near-surface layer of the ocean

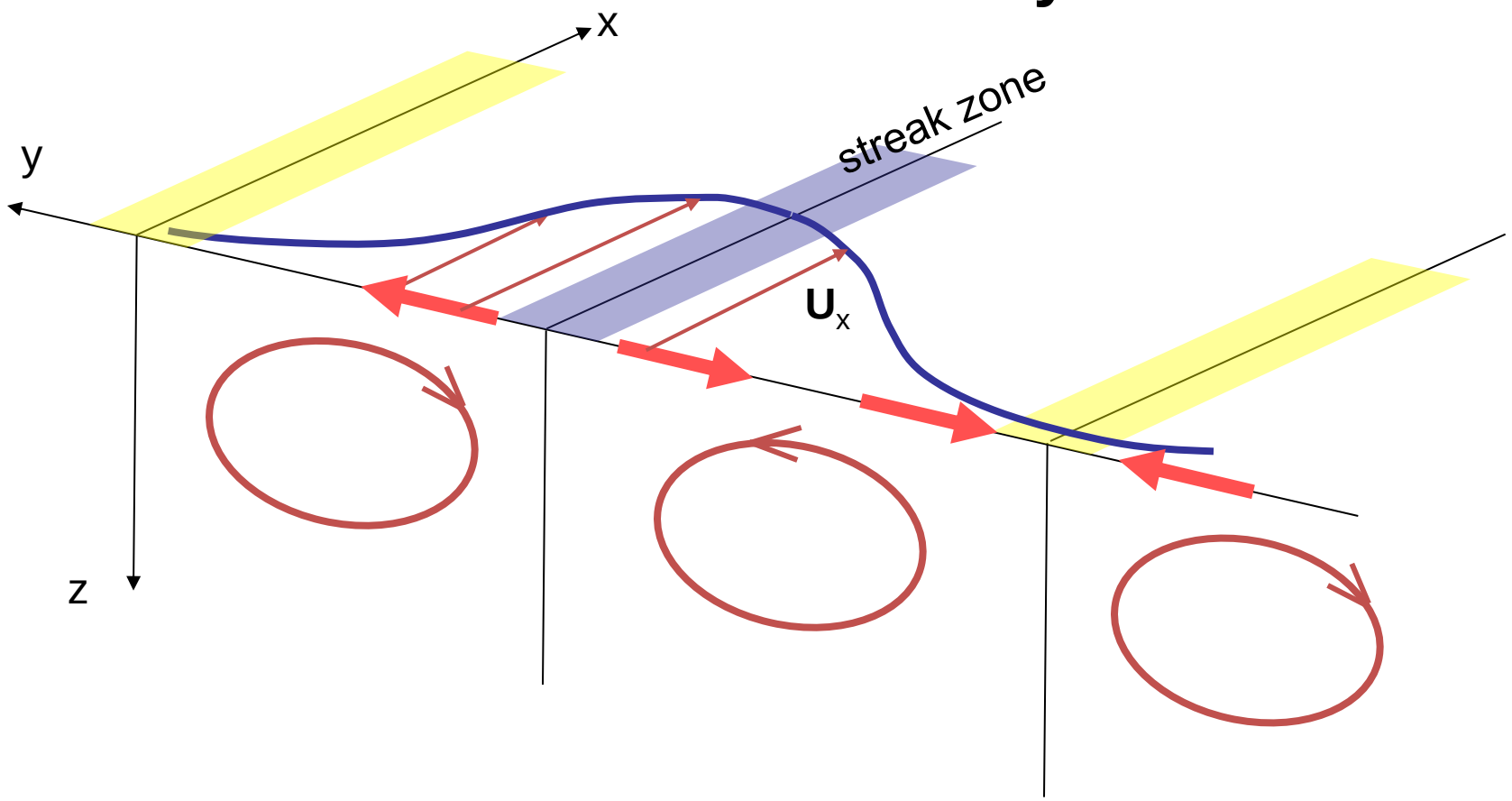

convergence, accumulation of surfactants

divergence, less surfactants

film stress

CFD Model Validation at UM RSMAS ASIST Tank

Soloviev, Matt, Gilman, Hühnerfuss, Haus, Jeong, Savelyev, and Donelan (2011)

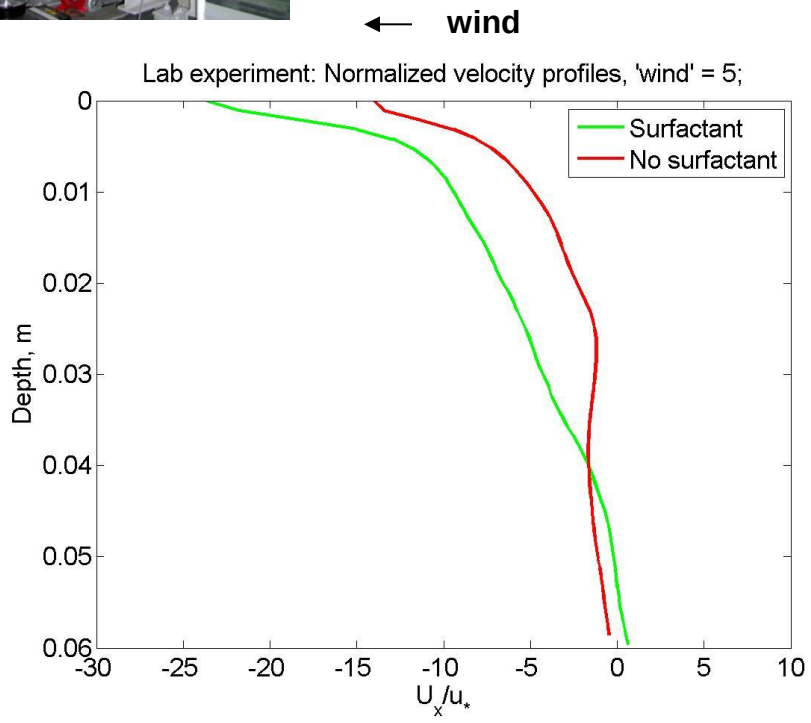

Average velocity profiles (DPIV) from lab experiment at ASIST

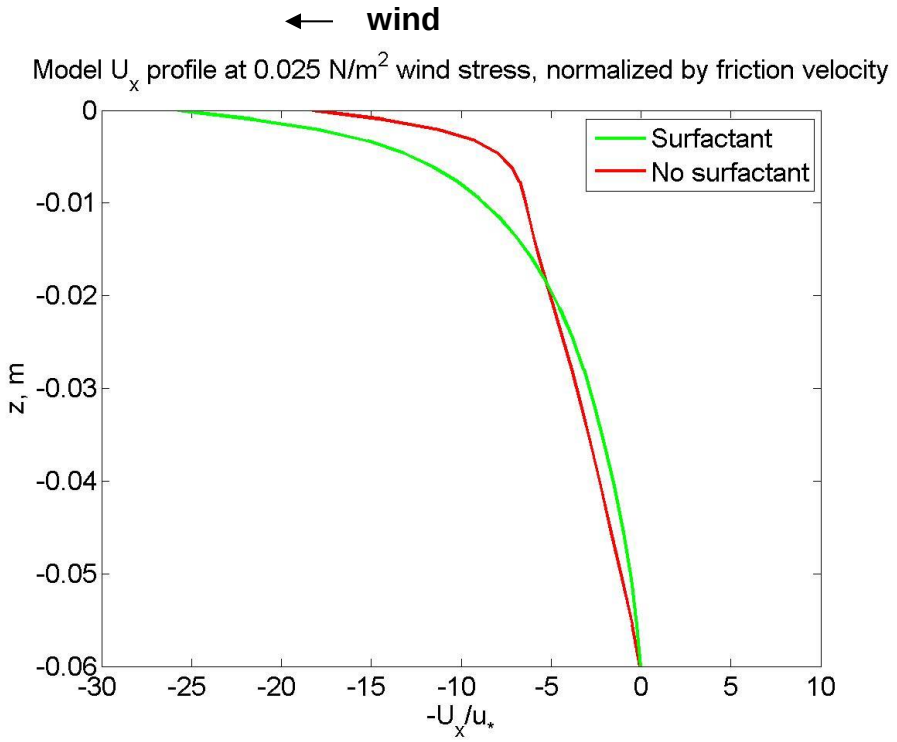

Average velocity profiles from CFD *Fluent* with visco-elastic surface boundary condition

Thermal Molecular Sublayer in Nighttime Conditions: Cool Skin

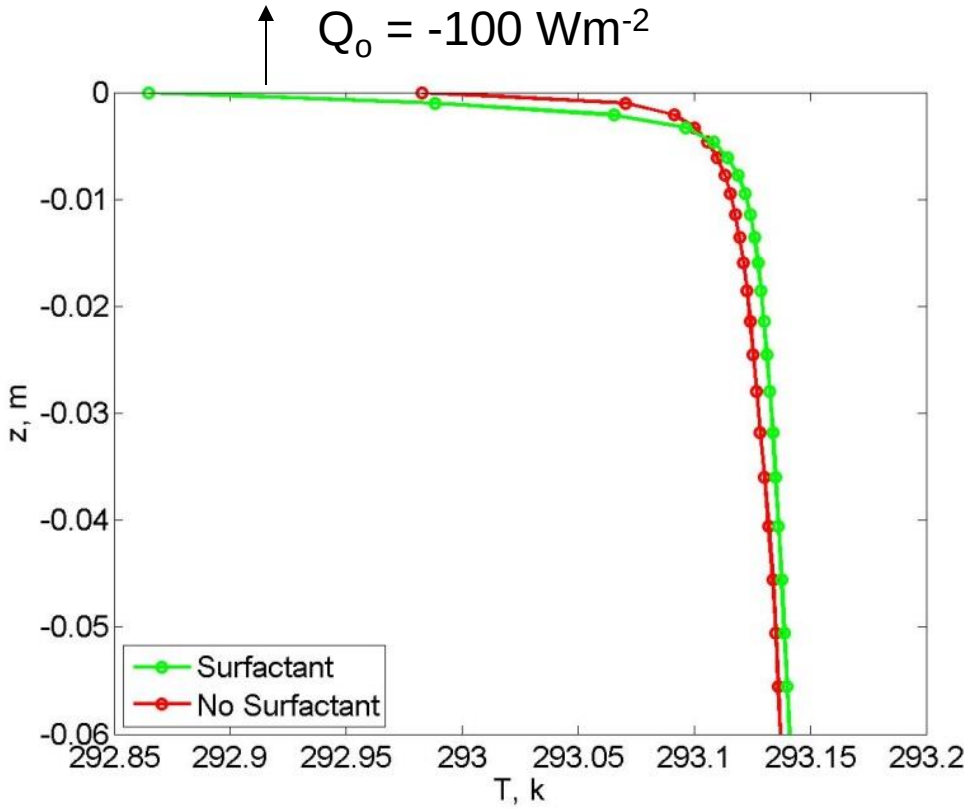

LES simulation:

U_{10} = 4 ms^{-1}

Pr = 10

In the presence of surfactant, ΔT changed from -0.15 K to -0.3 K

Matt et al. (2102)

Thermal Molecular Sublayer in Daytime Conditions Warm Skin

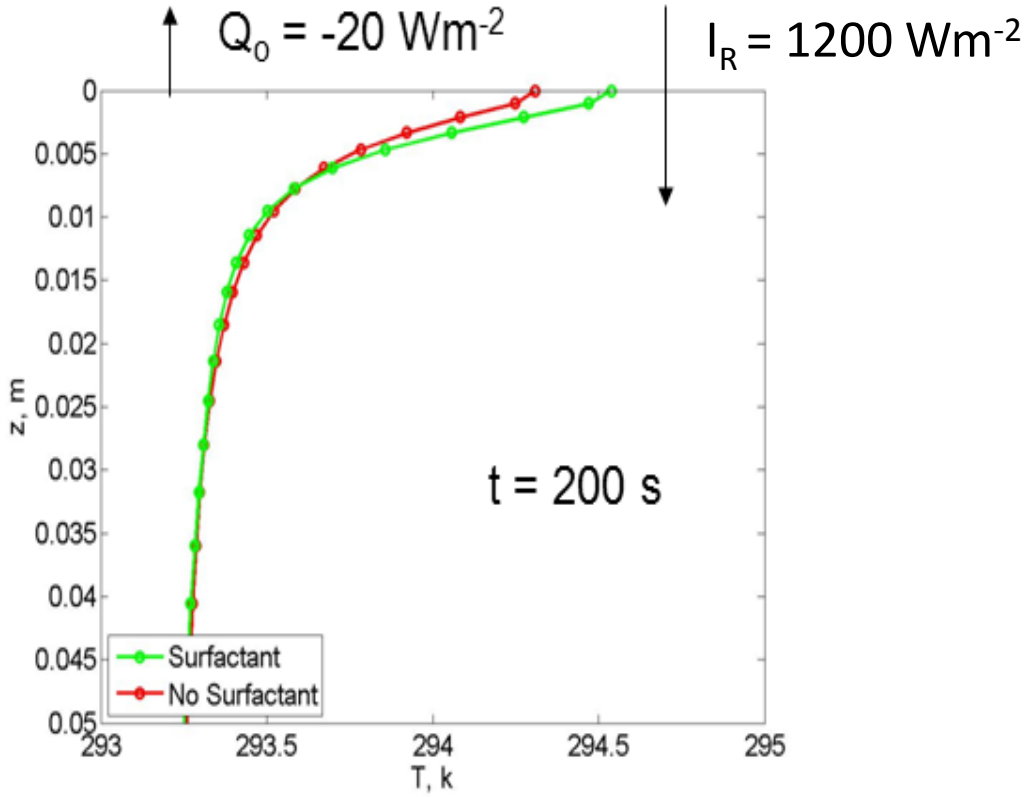

LES simulation:

U_{10} = 1 ms^{-1}

Pr = 10

Under strong solar irradiance, “cool skin” turns into a “warm skin”. Presence of surfactant increases temperature difference

Matt et al. (2102)

Chemical Structure of Slick- and Spill-forming Substances

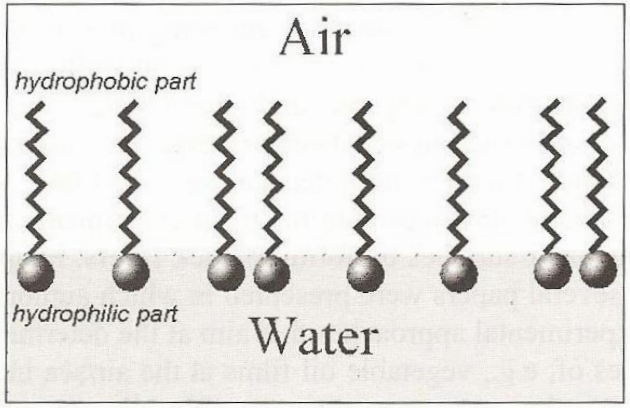

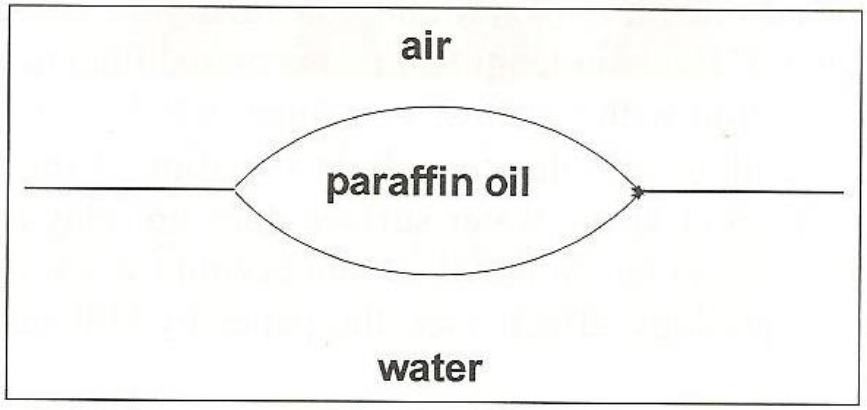

- Monomolecular surface film formed by surfactant
- 2.4-2.7 nm thickness
- Elastic damping

Paraffin oil on the water surface
μm to mm thickness
Viscous damping

Huehnerfuss (2008)

Turbulence damping below the air-sea interface may result in appreciable drop (nighttime) or increase (daytime) of the sea surface temperature in slick or oil spill areas

Can Near-Surface Temperature Gradients and Surface Roughness Changes Induce Motion of Surface Oil?

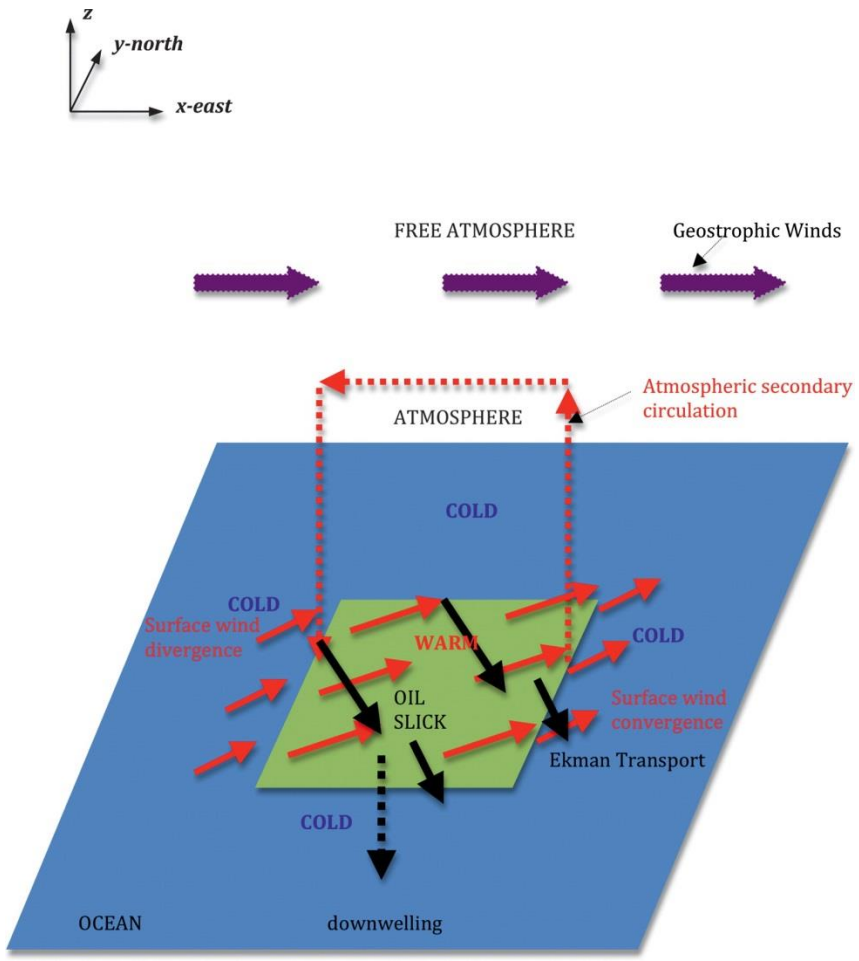

"3D schematic diagram depicting the induced atmospheric secondary circulation and downwelling of oil under the influence of SST gradient in the boundary between an oil slick (green shading) and water (blue shading). Oil slick temperature is spatially homogeneous and higher than the water temperature, which is also spatially homogeneous. Near-surface air temperature is 0.5°C lower than SST in the waterand the oil slick.

Red solid arrows denote surface winds at 10 m above the sea surface. Red dashed arrows denote the induced atmospheric secondary circulation. Black solid arrows denote the resultant Ekman transport in the boundary between the water and the oil slick. Black dashed arrows denote the downwelling of the oil slick owing to the net Ekman transport within the boundary…"

(Zheng, Bourassa, and Highes, 2013)

Turbulence and Fine Structure

Small-Scale Measurements in the Near-Surface Layer of the Ocean during TOGA COARE

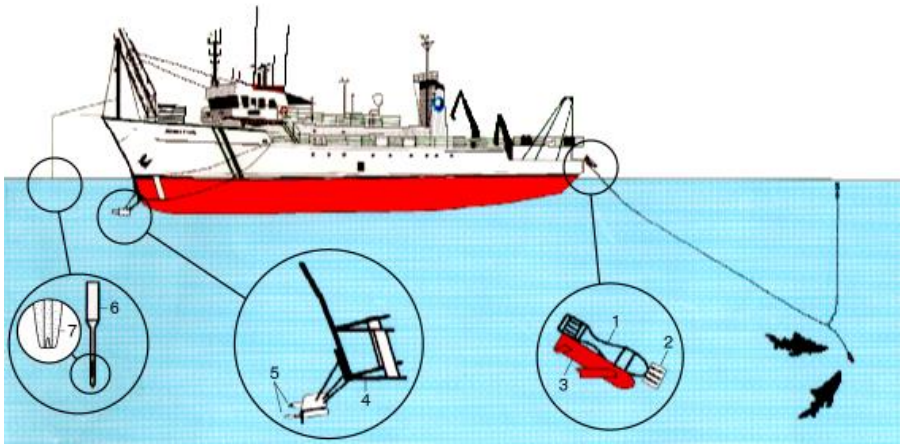

1 - free-rising profiler coupled with carrier; 2- temperature, conductivity and fluctuation-velocity probes on free-rising profiler; 3 - carrier; 4 - bow frame; 5 - bow units (temperature, conductivity, pressure sensor; fluctuation-velocity, tilt sensor); 6 – dropsonde; 7 - temperature probe of micro-wire type.

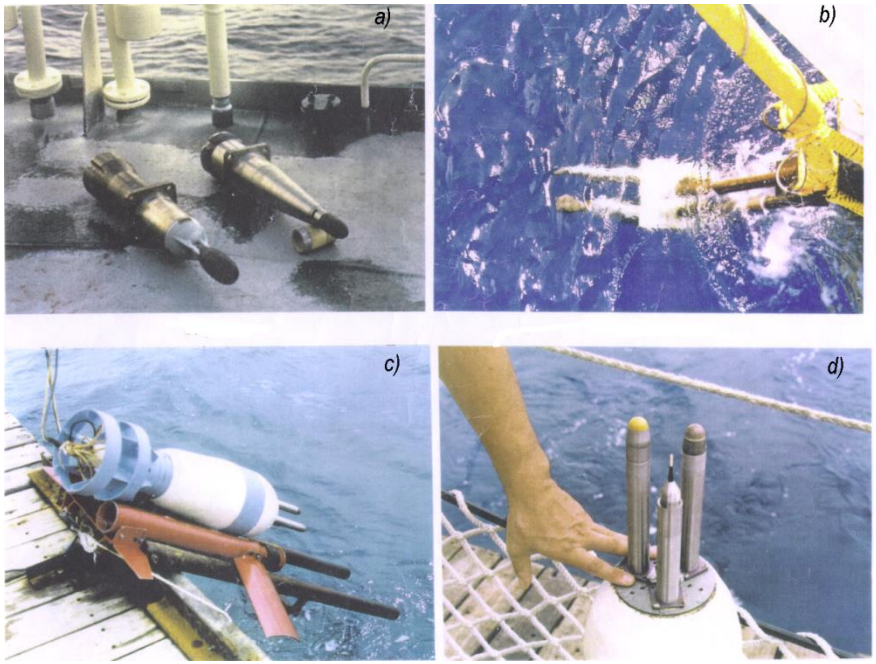

Photo of bow sensors (a and b) and free-rising profiler (c and d).

Soloviev and Luks (2006)

Wave-Breaking Turbulence

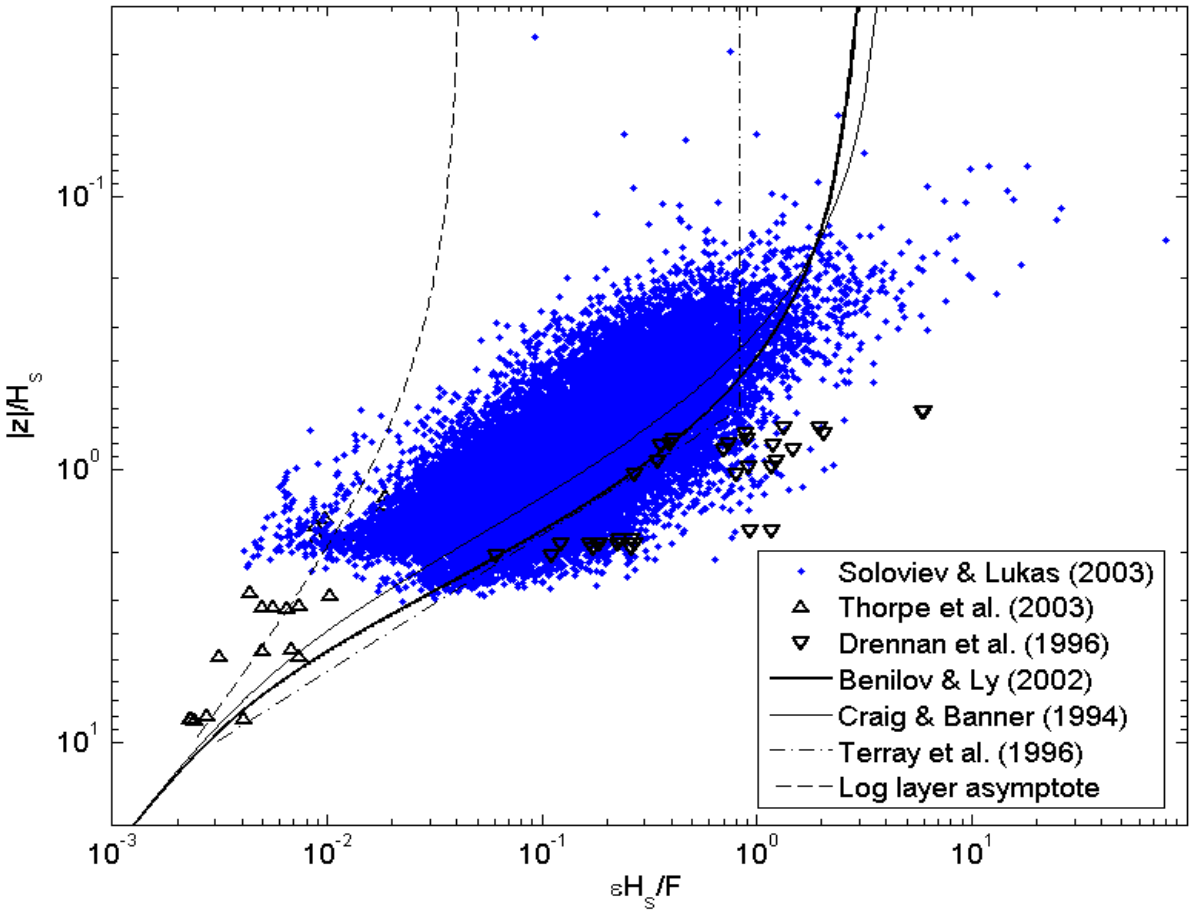

ε – dissipation rate of TKE
H_s – significant wave height
F -flux of TKE from waves to turbulence
z – depth (distance from the surface)

Soloviev and Lukas (2006)

Mixing coefficient in the wave-enhanced turbulent boundary layer (continuous line) in comparison with the logarithmic layer prediction (dashed line)

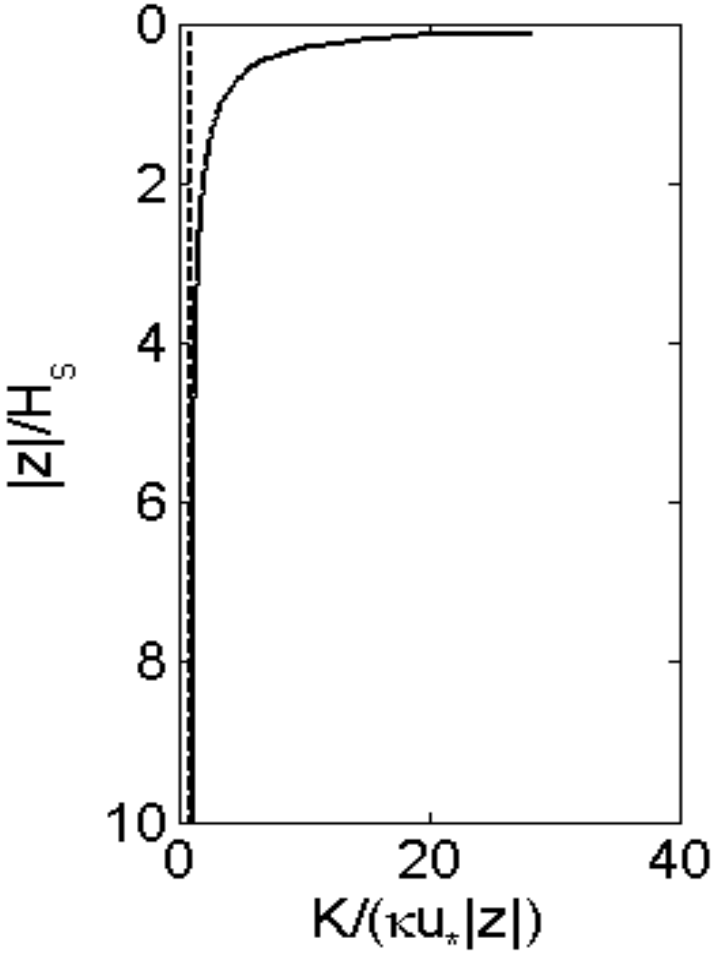

K – vertical mixing coefficient
H_s – significant wave height
z – depth (distance from the surface)
u_*- frictional velocity in water
κ–von Karman's constant

Soloviev and Lukas (2006)

Effect of Stratification

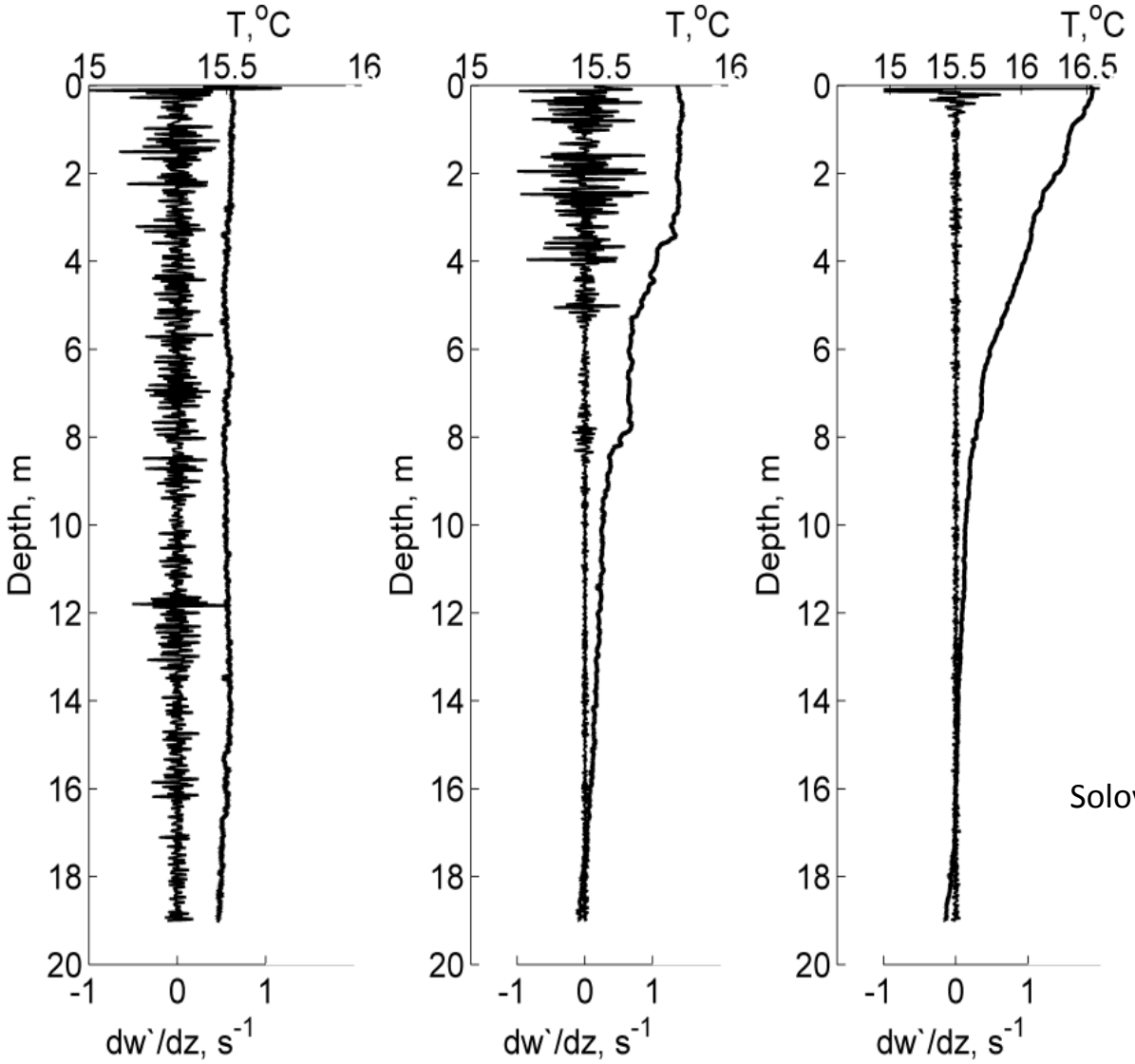

Soloviev and Lukas (2006)

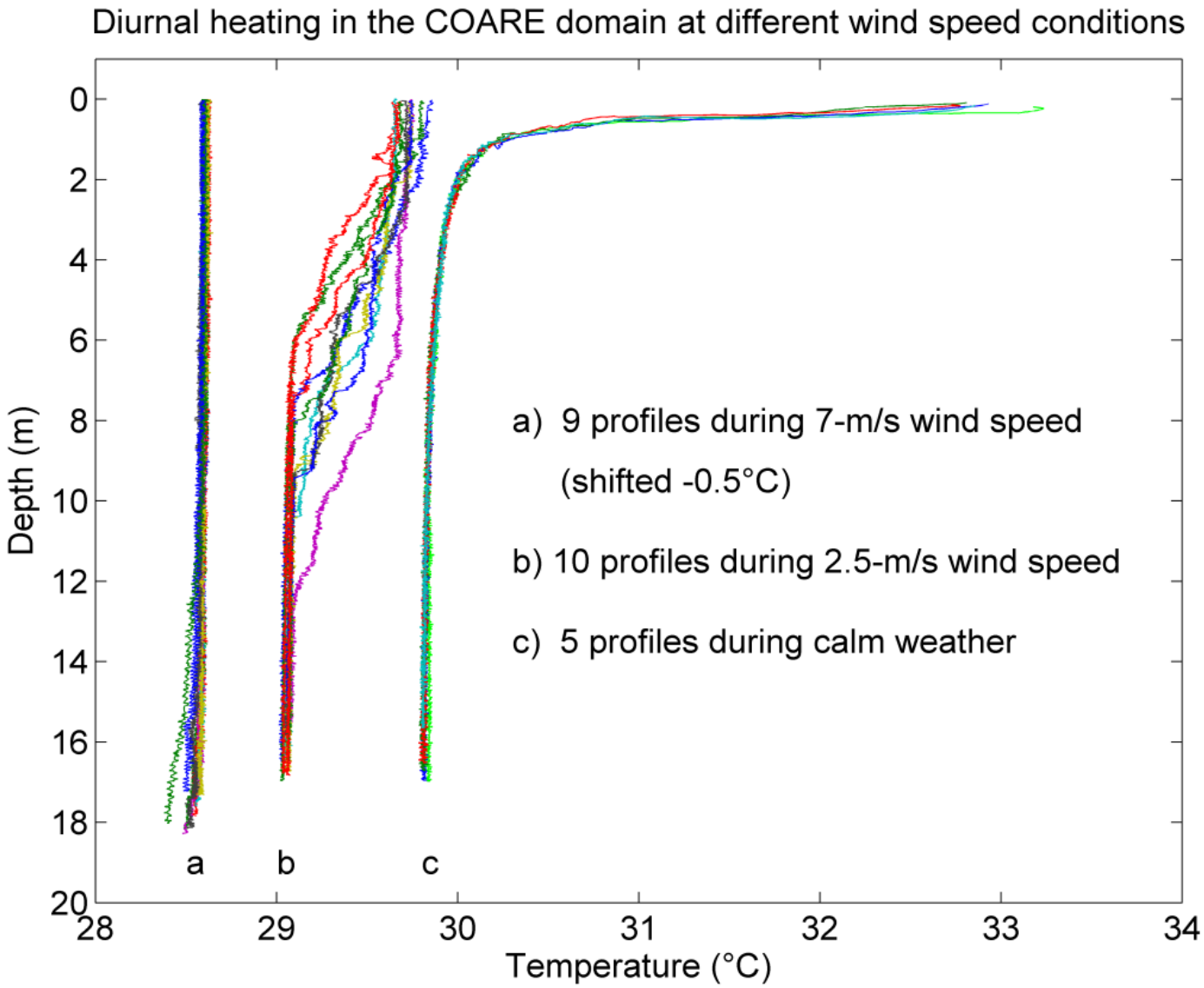

Soloviev and Lukas (2006)

Spatial Variability of Diurnal Thermocline

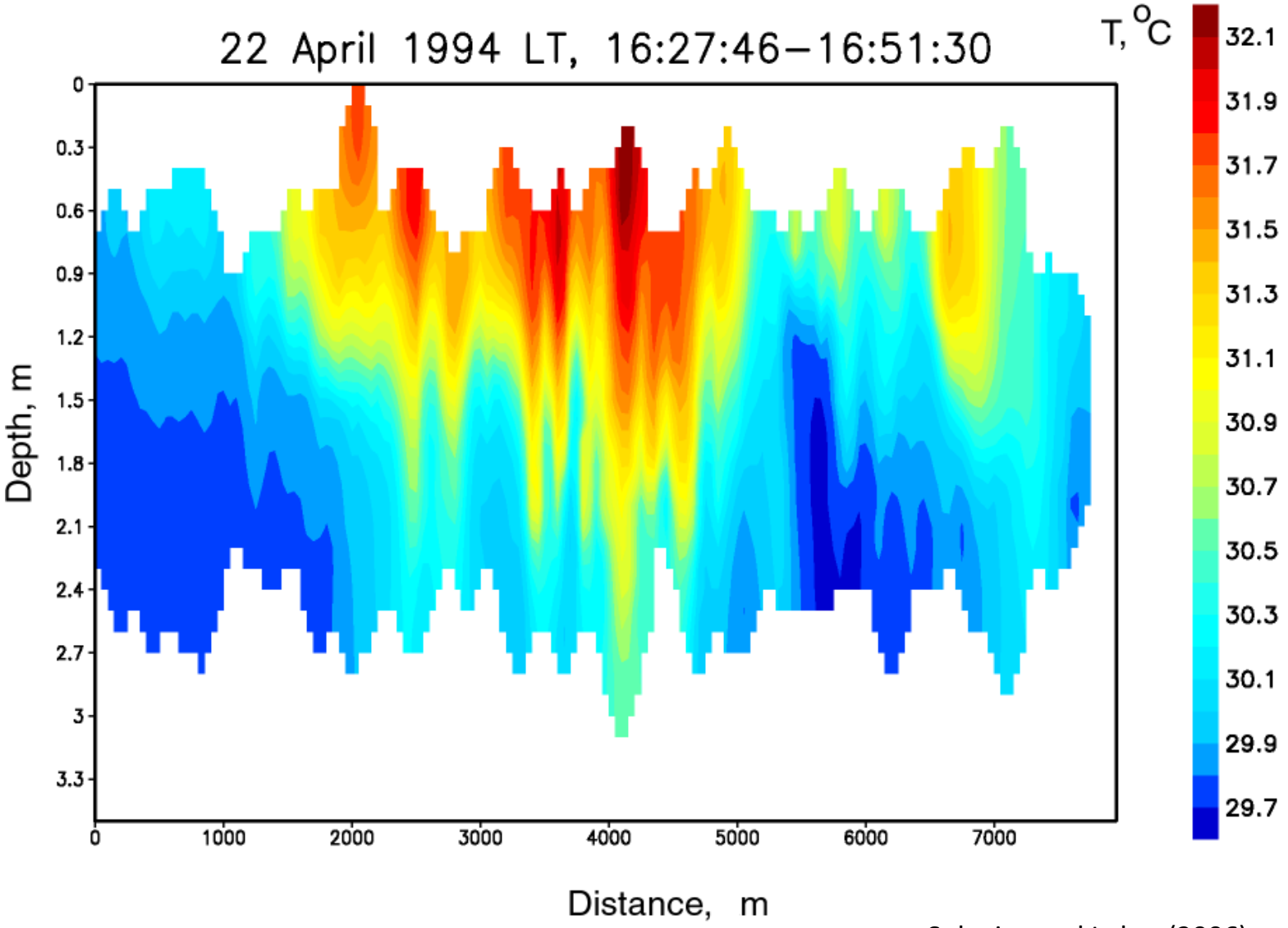

Soloviev and Lukas (2006)

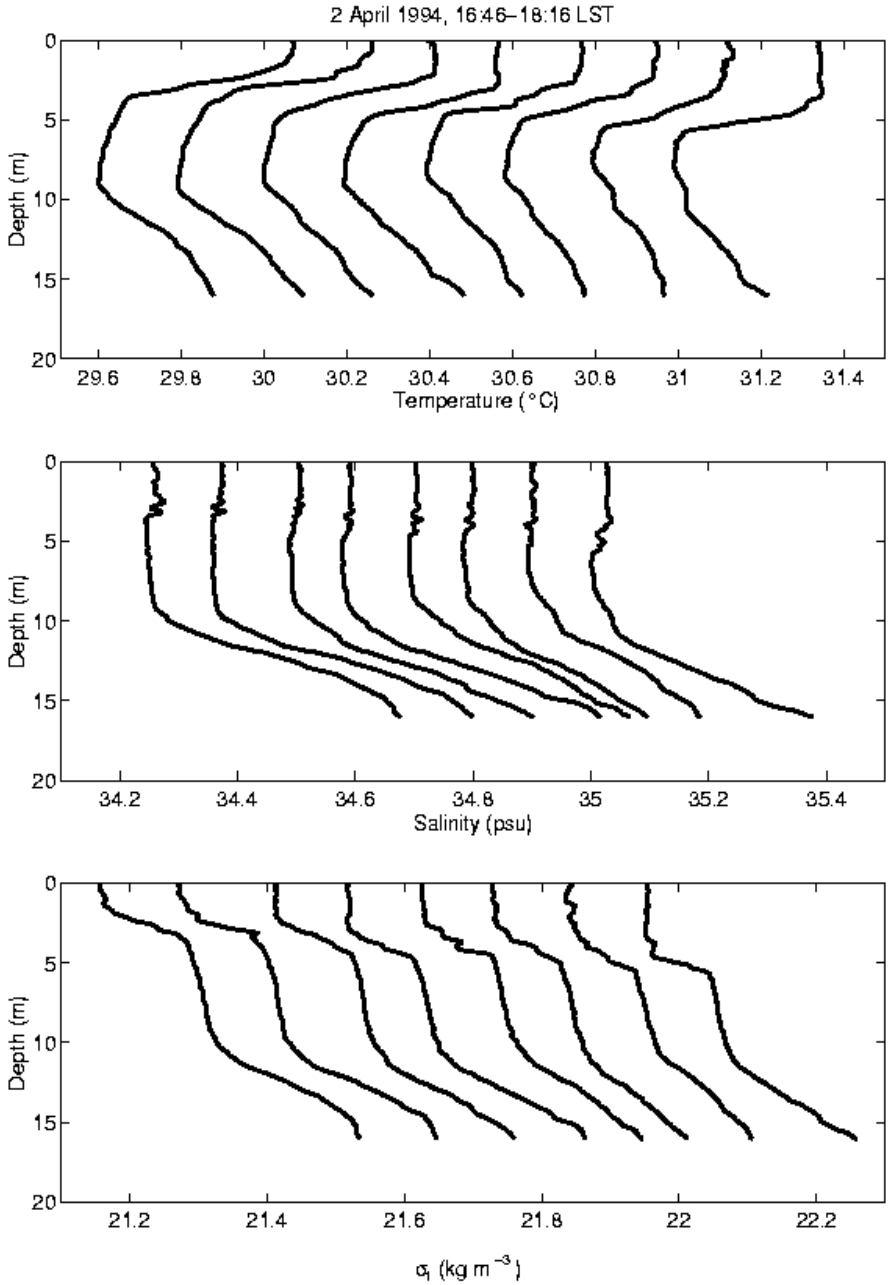

Rain-formed stratification traps heat in the near-surface layer

Soloviev and Lukas (2006)

Surface Intensified Jets

Idealized situation:

- Wind stress and stabilizing buoyancy flux at the ocean surface
- Depth of the mixed layer h_D is proportional to the Oboukhov length scale, L_0

$$h_D \sim L_O = u_*^3 / \left[\kappa \alpha_T g Q_n / \left(c_p \rho \right) \right] = C_{10}{}^{3/2} U_{10}{}^3 / \left[\kappa \alpha_T g Q_n / \left(c_p \rho \right) \right]$$

$$\Delta T = \frac{-Q_n t}{c_p \rho h_D} \sim \frac{-Q_n t}{c_p \rho L_O} = \frac{-\alpha_T g \kappa}{u_*{}^3} \left(\frac{Q_n}{c_p \rho} \right)^2 t = \frac{-\alpha_T g \kappa}{C_{10}^{3/2}} \left(\frac{Q_n}{c_p \rho} \right)^2 U_{10}{}^{-3} t$$

$$\Delta u = \frac{\tau_0 t}{\rho h_D} \sim \frac{\tau_0 t}{\rho L_O} = \frac{\kappa \alpha_T g Q_n}{c_p \rho u_*} t = \frac{\kappa \alpha_T g Q_n}{c_p \rho C_D^{1/2}} U_{10}{}^{-1} t$$

Surface Intensified Diurnal Jet

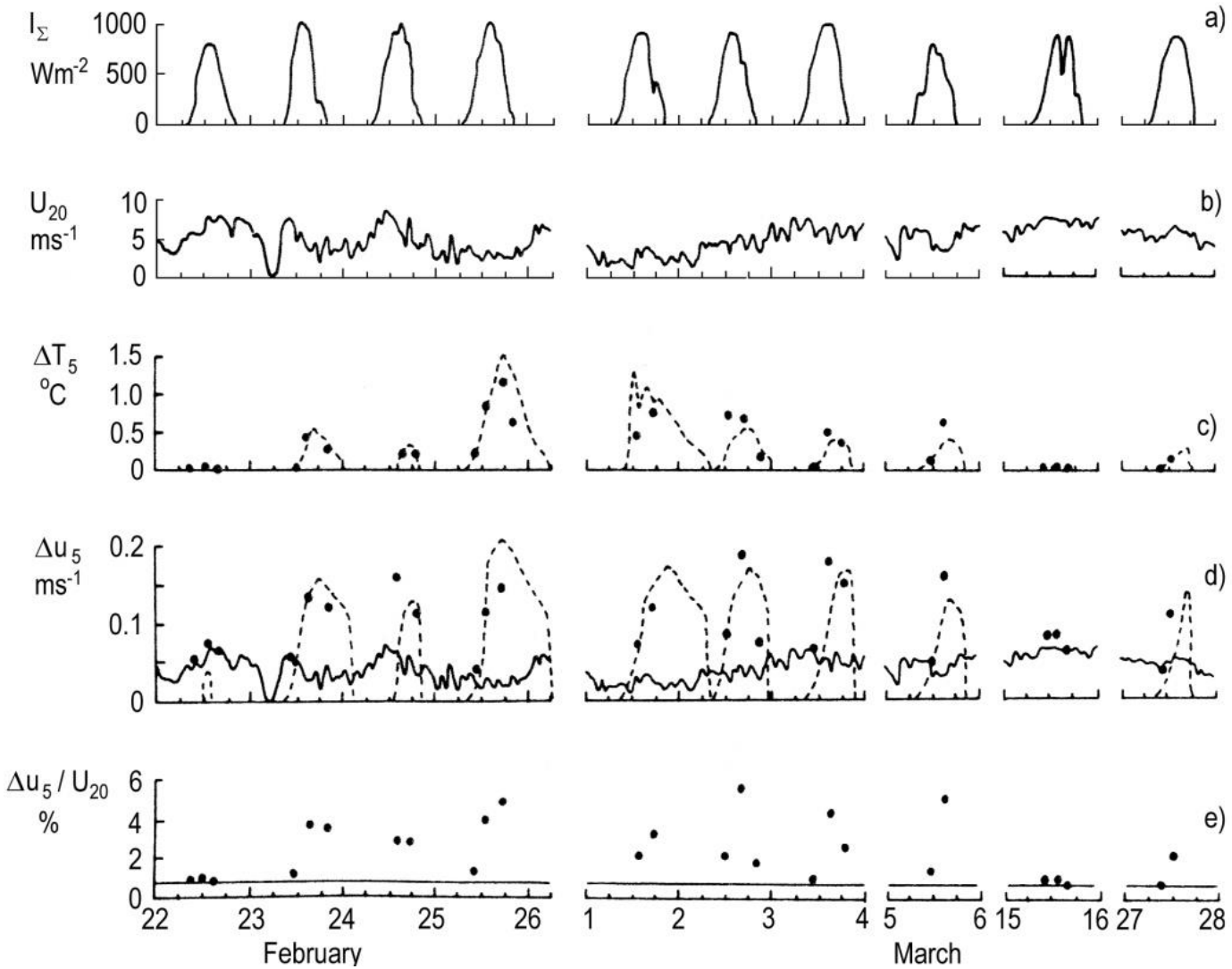

Kudryavtsev and Soloviev (1990)

Slipper Near-surface Layer

$$C_u = \left(u_* / \Delta u_5\right)^2$$

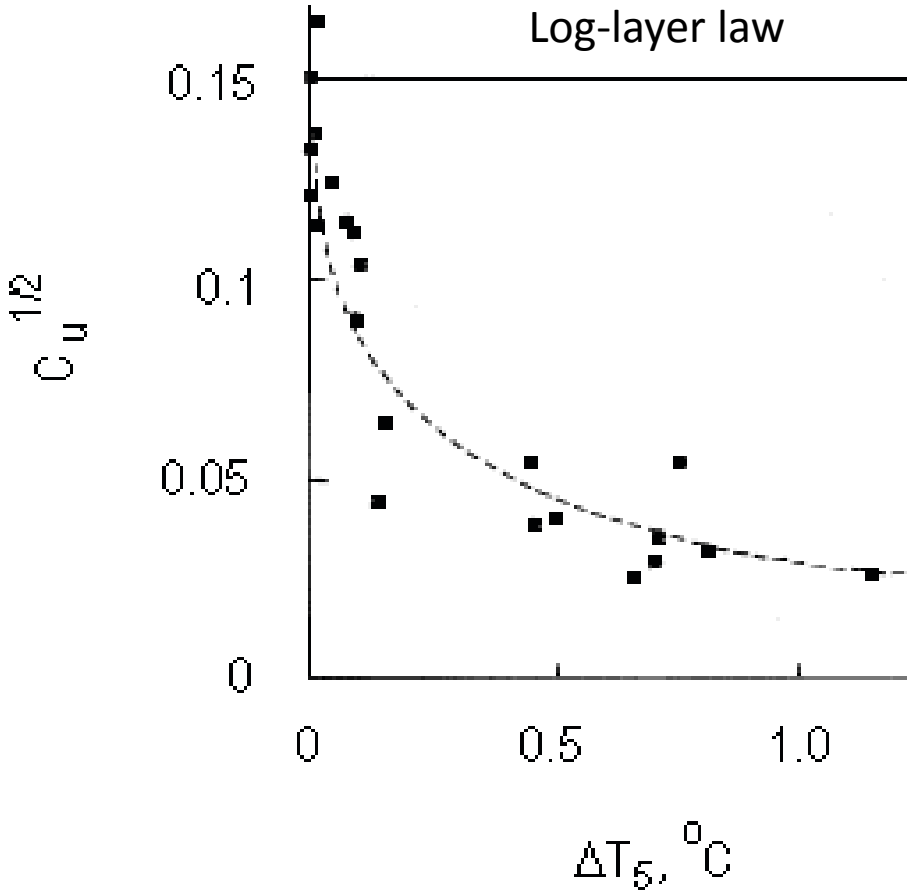

Dependence of the drag coefficient in the near-surface layer of the ocean on the temperature difference across the diurnal thermocline during a period of intense warming (morning and noon hours).

Kudryavtsev and Soloviev (1990)

Upper Velocity Limit for Surface Intensified Jets

Diurnal jet:

$$\Delta u_{\max} = \left[-2Ri_{cr}^{-1} \alpha_T g \Upsilon_D / \left(c_p \rho \right) \right]^{1/2} \approx 0.3 \text{ m/s}$$

$$\Upsilon_D = \int_0^t \left[\left(1 - A \right) I_\Sigma - Q_0 \right] dt' \text{ - cumulative heat}$$

Rain-formed jet:

$$\Delta u_{\max} = \left[2Ri_{cr}^{-1} \beta_S g S_0 M_r \right]^{1/2} \approx 0.5 \text{ m/s}$$

$$M_r = \int_0^t P dt' \text{ - cumulative precipitation}$$

Coherent Structures

Sharp frontal interfaces

Soloviev et al. (2002)

Sharp frontal interfaces

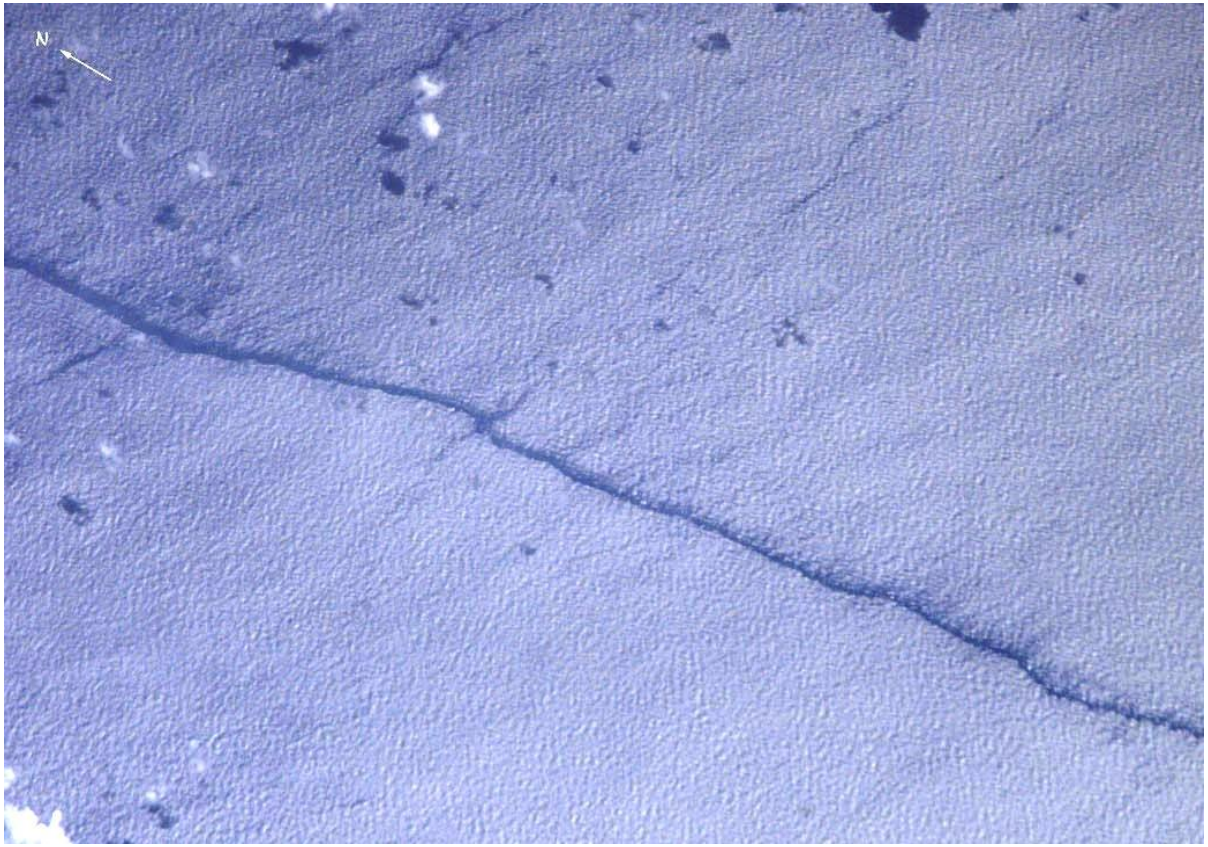

An image taken from International Space Station on May 24, 2001 in the Equatorial Pacific (2.3^{o}N 159.1^{o}E)

Soloviev and Lukas (2006)

Spirals on the ocean surface from the collection of Stevenson (1985)

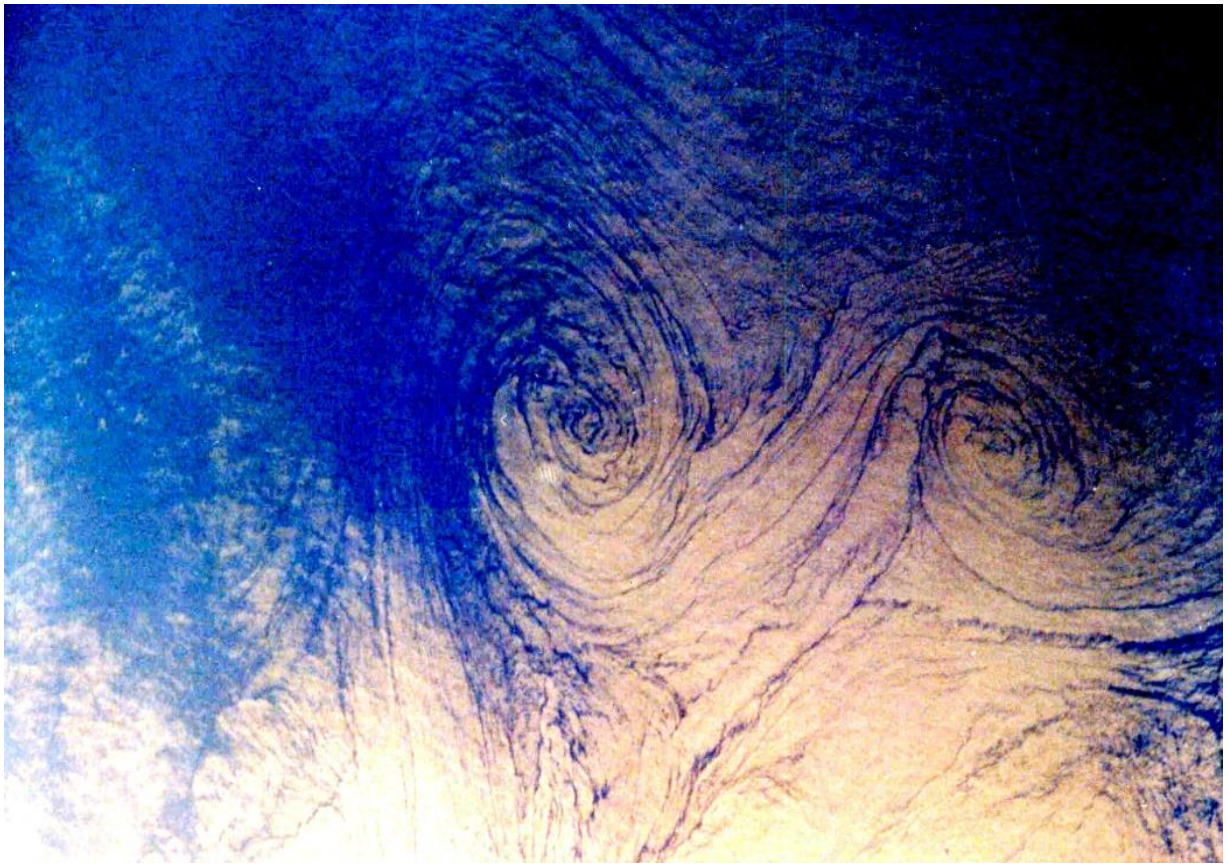

Sharp Frontal Interface in the Western Equatorial Pacific

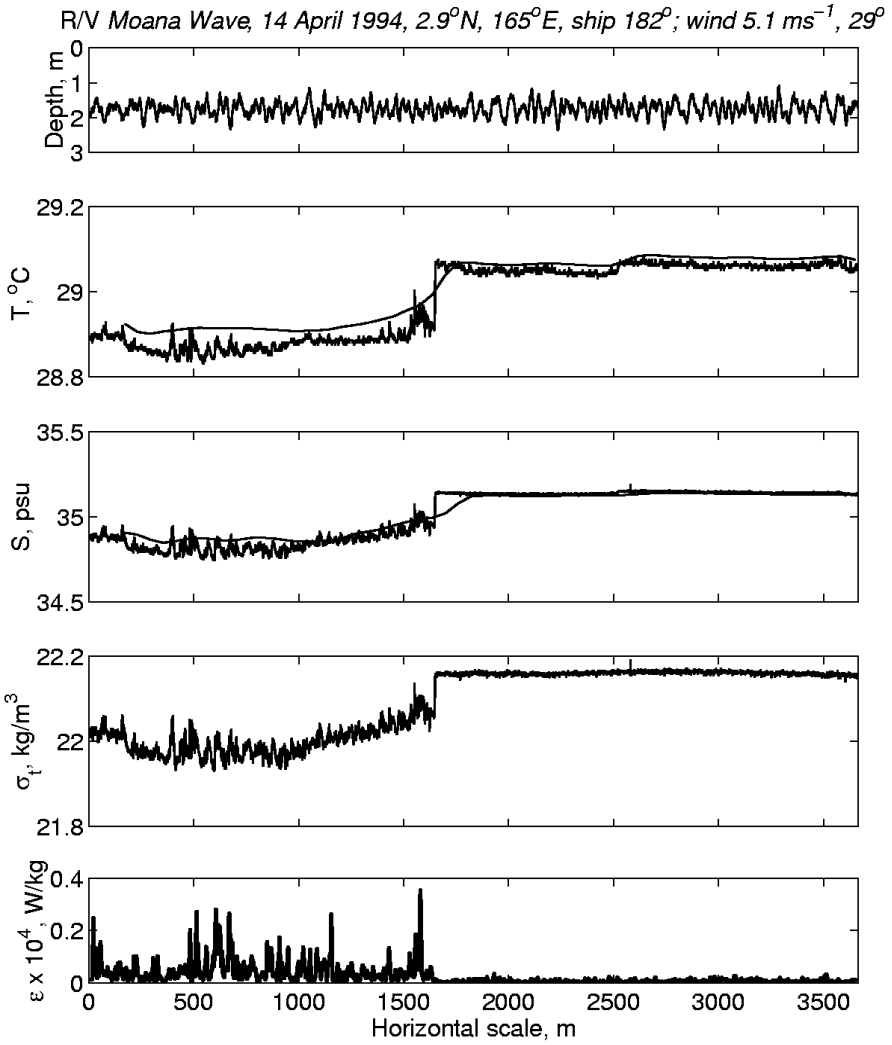

Soloviev and Lukas (2006)

Directional Anisotropy of Sharp Frontal Interfaces Relative to Wind Velocity

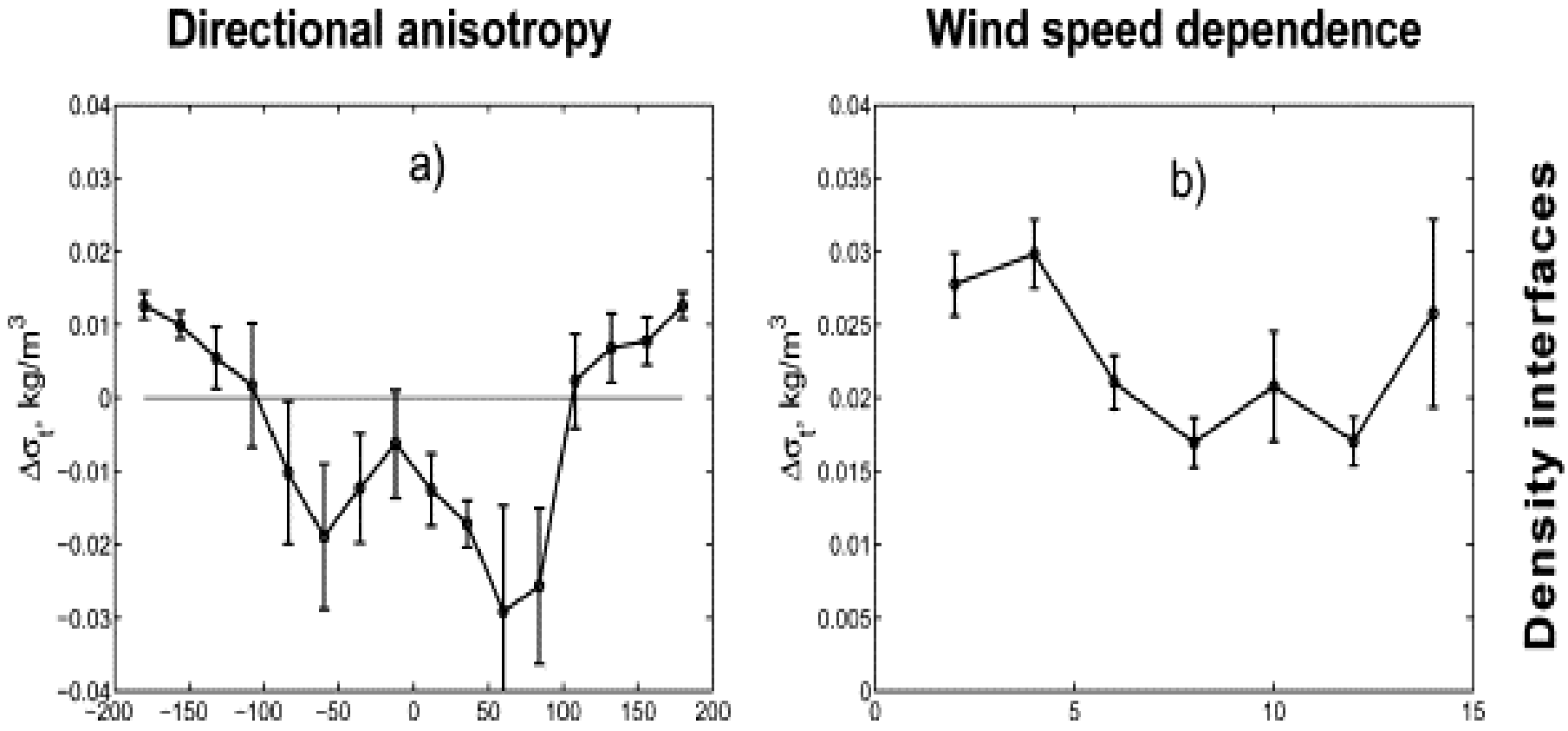

Soloviev and Lukas (2006)

Stommel's Overturning Gate: Interaction of a sharp frontal interface with wind stress?

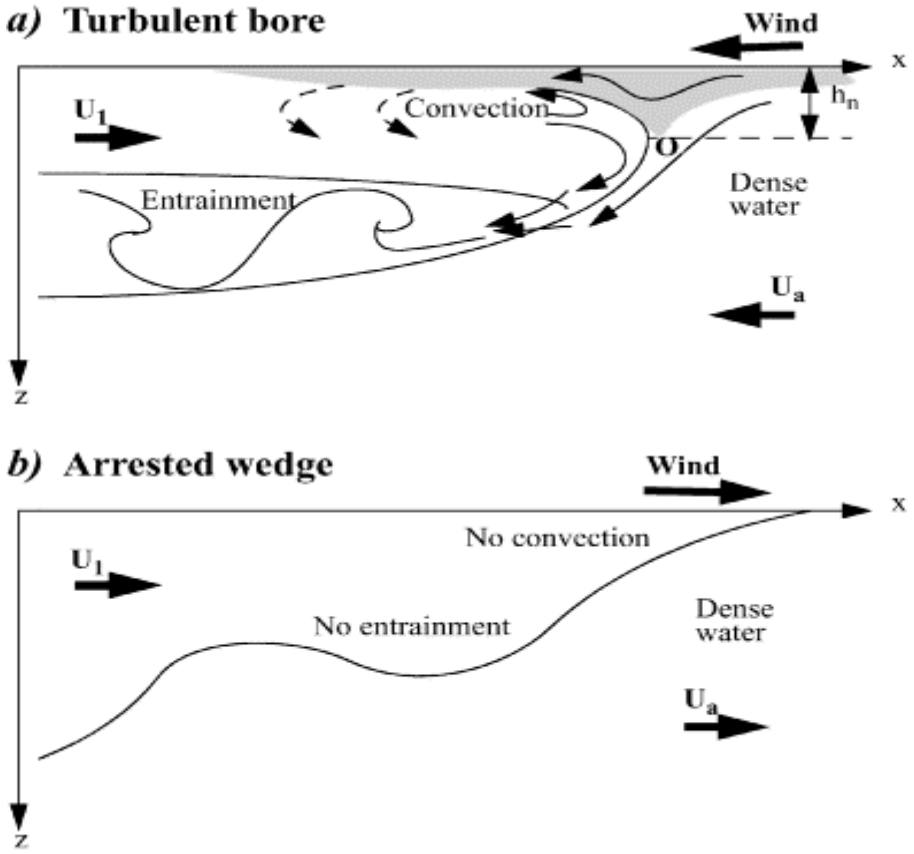

May work on sharp interfaces, less than 100 m wide.

Ramp-like Structures

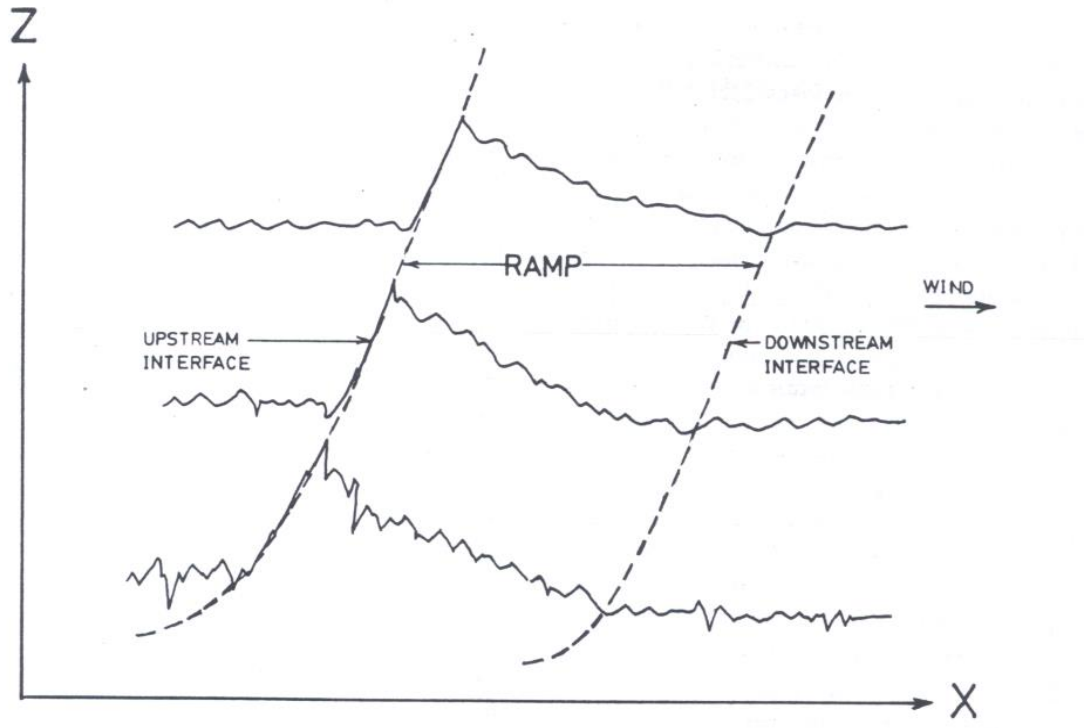

Phong-Anant et al. (1980) schematic representation of temperature ramps in the atmospheric boundary layer

Ramp-like Structures in the Near-surface Ocean

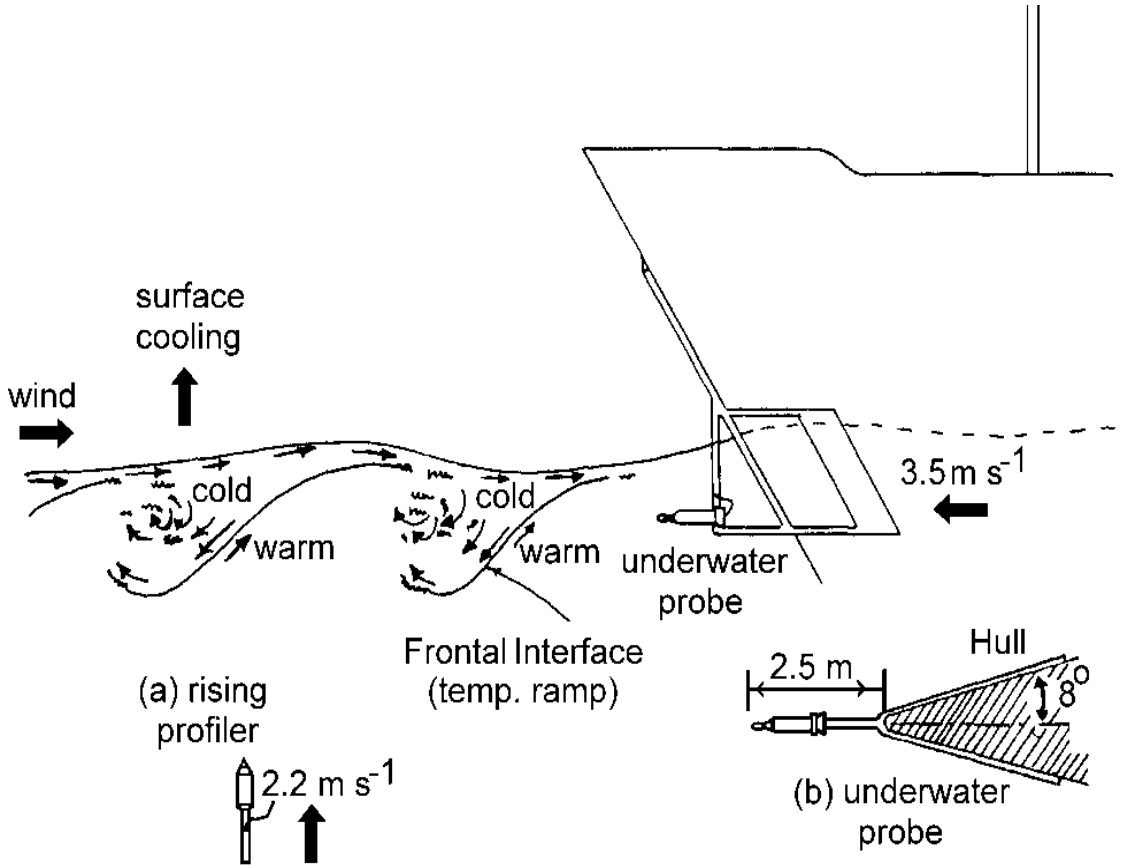

Schematic representation showing spatially coherent organized motion in the upper ocean boundary layer under unstably stratified conditions (Soloviev, 1990)

Ramp-like structures

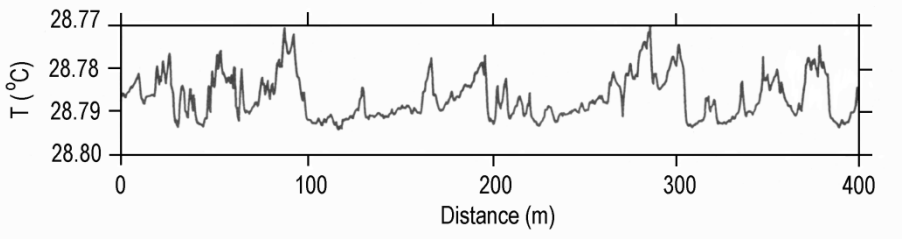

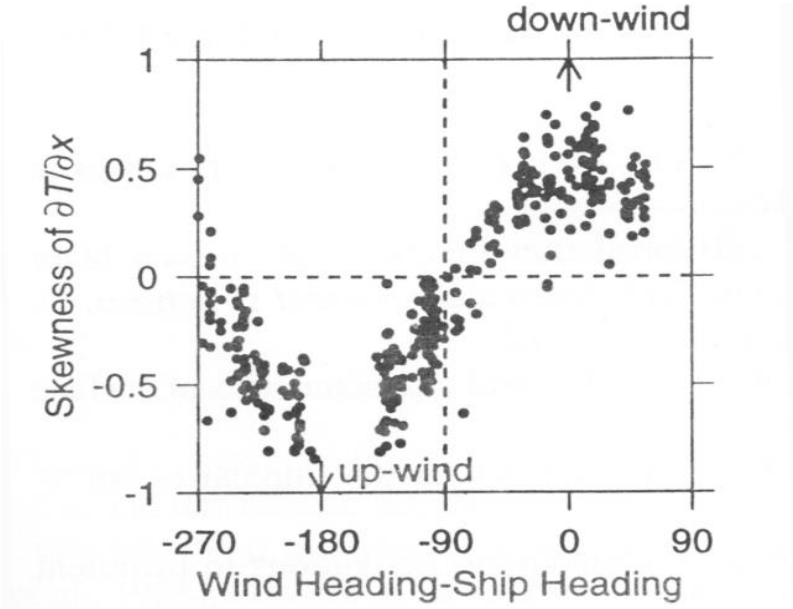

Skewness of $\partial T/\partial x$ versus the relative angle between the wind and ship heading under unstably stratified conditions in the western equatorial Pacific Ocean. After Wijesekera et al. (1999).

Langmuir Circulation

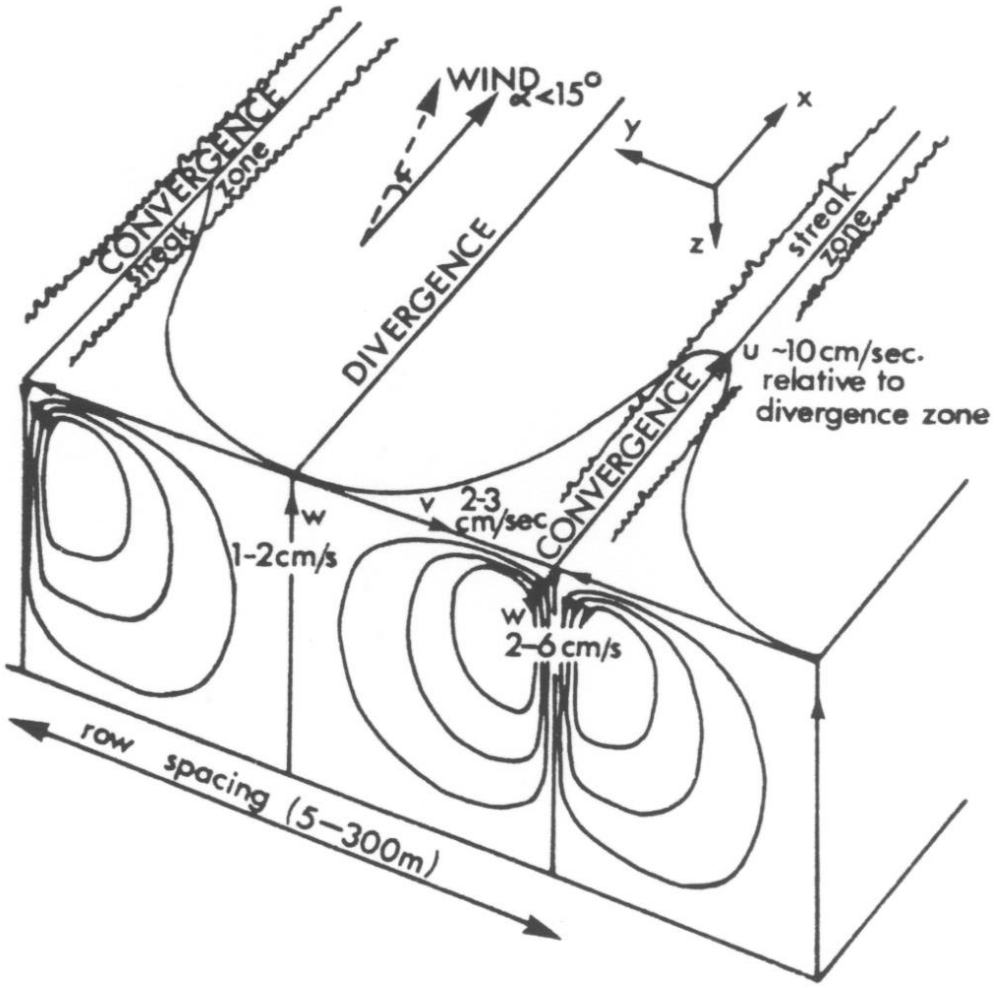

Pollard's (1979) sketch of Langmuir circulations

Free Convection

Shadowgraph picture of the development of secondary haline convection. Foster (1975).

Free Convection

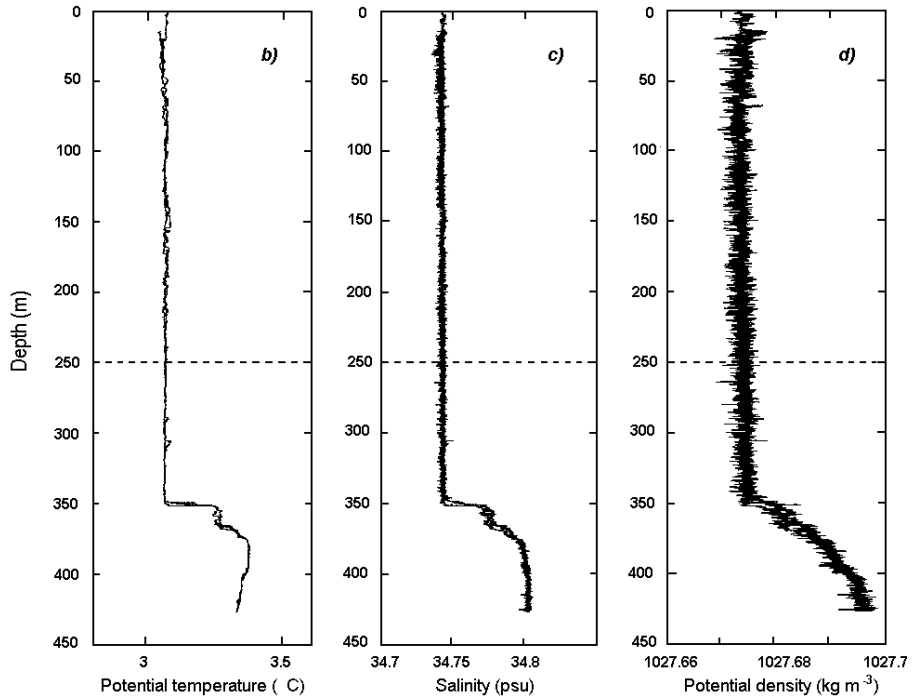

Zhang et al. (2001).

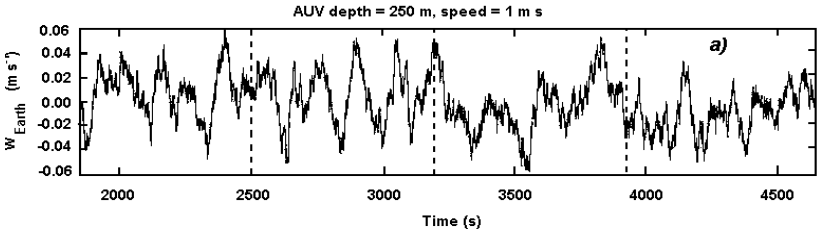

The vertical flow velocity at 250 m depth measured during an autonomous underwater vehicle (AUV) mission in the Labrador Sea.

High Wind Speed

Local Perturbation of the KH Instability

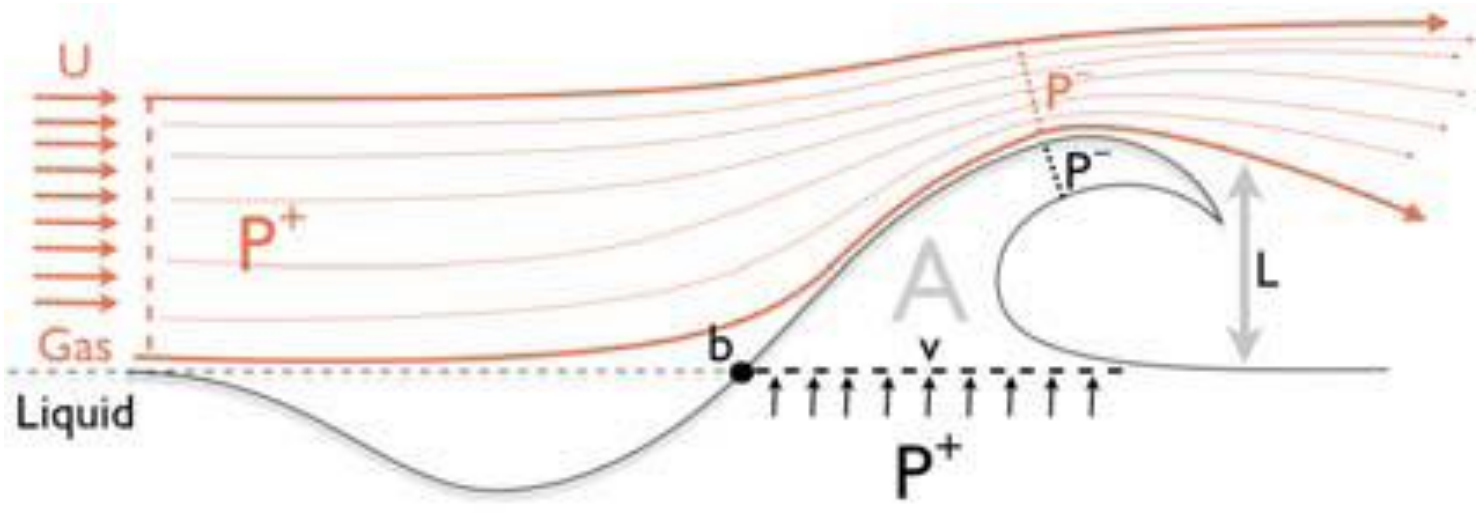

ρ_a

ρ_w

Hoepffner, Blumenthal, and Zaleski (2011)

Acceleration of the air stream above a short wave induces a pressure drop:

$$\Delta P = P^{+} - P^{-} = \rho_a U^2 k L .$$

The instability breaks up the interface if ΔP exceeds the combined restoring force of gravity and surface tension:

$$\Delta P > (\rho_w g + \sigma_s k^2) L ,$$

σ_s the surface tension, k the wavelength.

Numerical Simulations

• In order to demonstrate the possibility of the direct disruption of the air-sea interface under hurricane conditions, we used an idealized 3D VOF-LES model set-up.

• A series of numerical experiments has been conducted using the computational fluid dynamics software ANSYS/Fluent (Soloviev et al., 2012).

• Wind stress was applied at the upper boundary of the air layer, ranging from no wind stress to hurricane force wind stress.

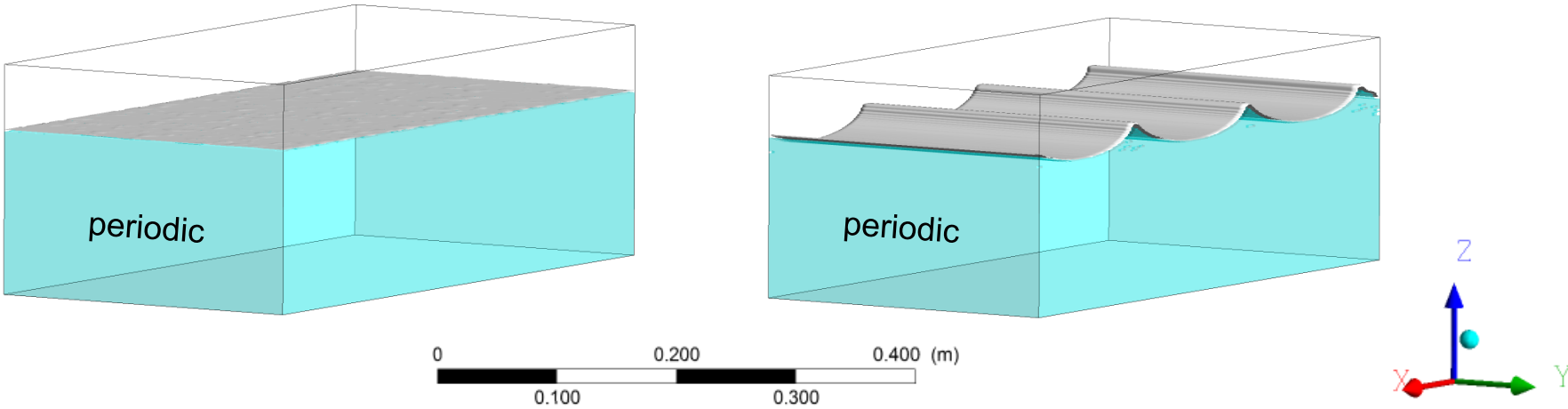

3D Simulation of Air-Water Interface in Hurricane Conditions: Volume Fraction –Side View

Wind stress 4 N m^{-2} (U_{10} =40 m/s)

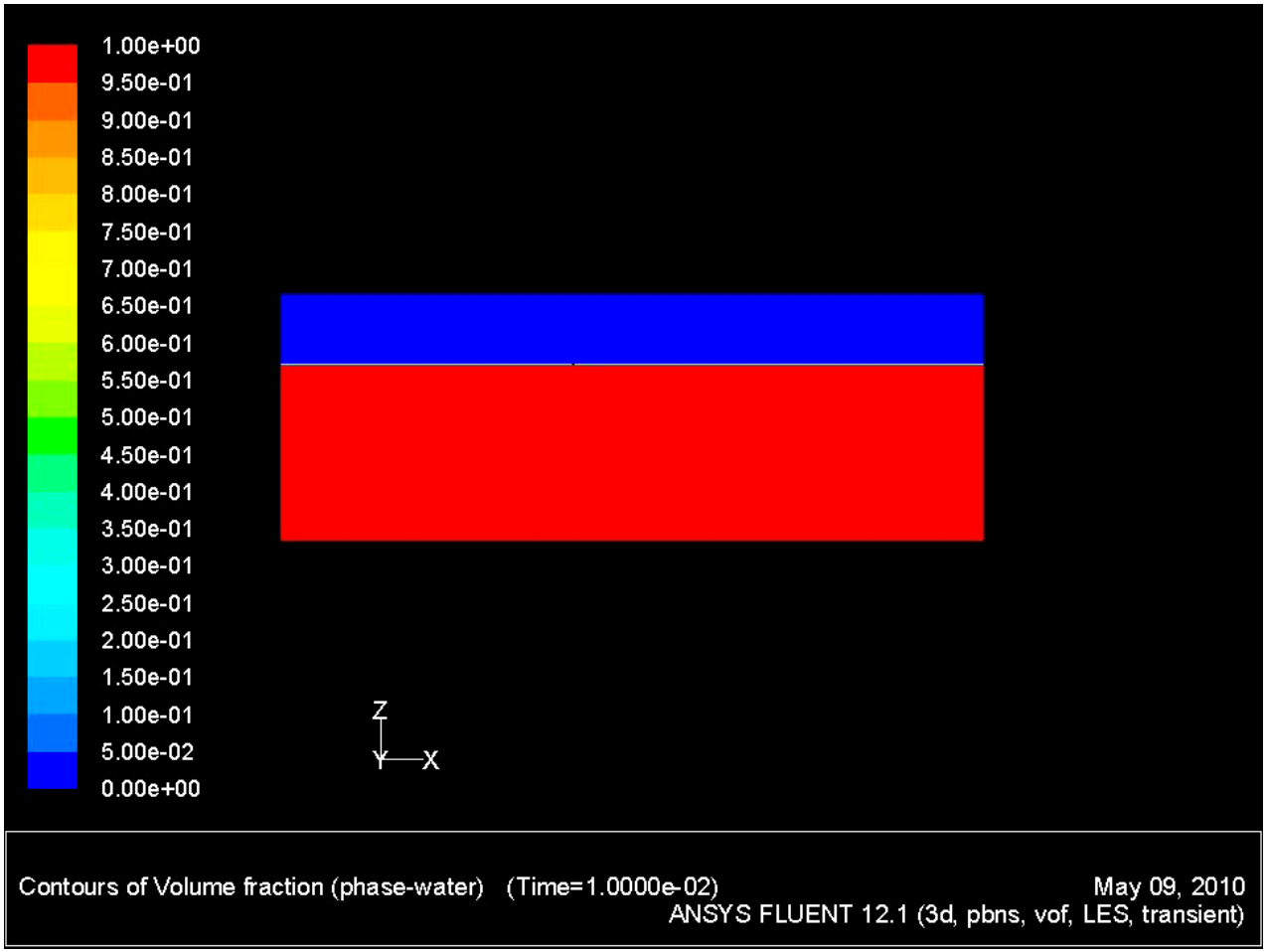

Fluent: VOF LES WALE. Domain size: 1 m X 0.5 m X 0.3 m

“Projections” from the air-water interface initiate production of large spray particles in strong winds

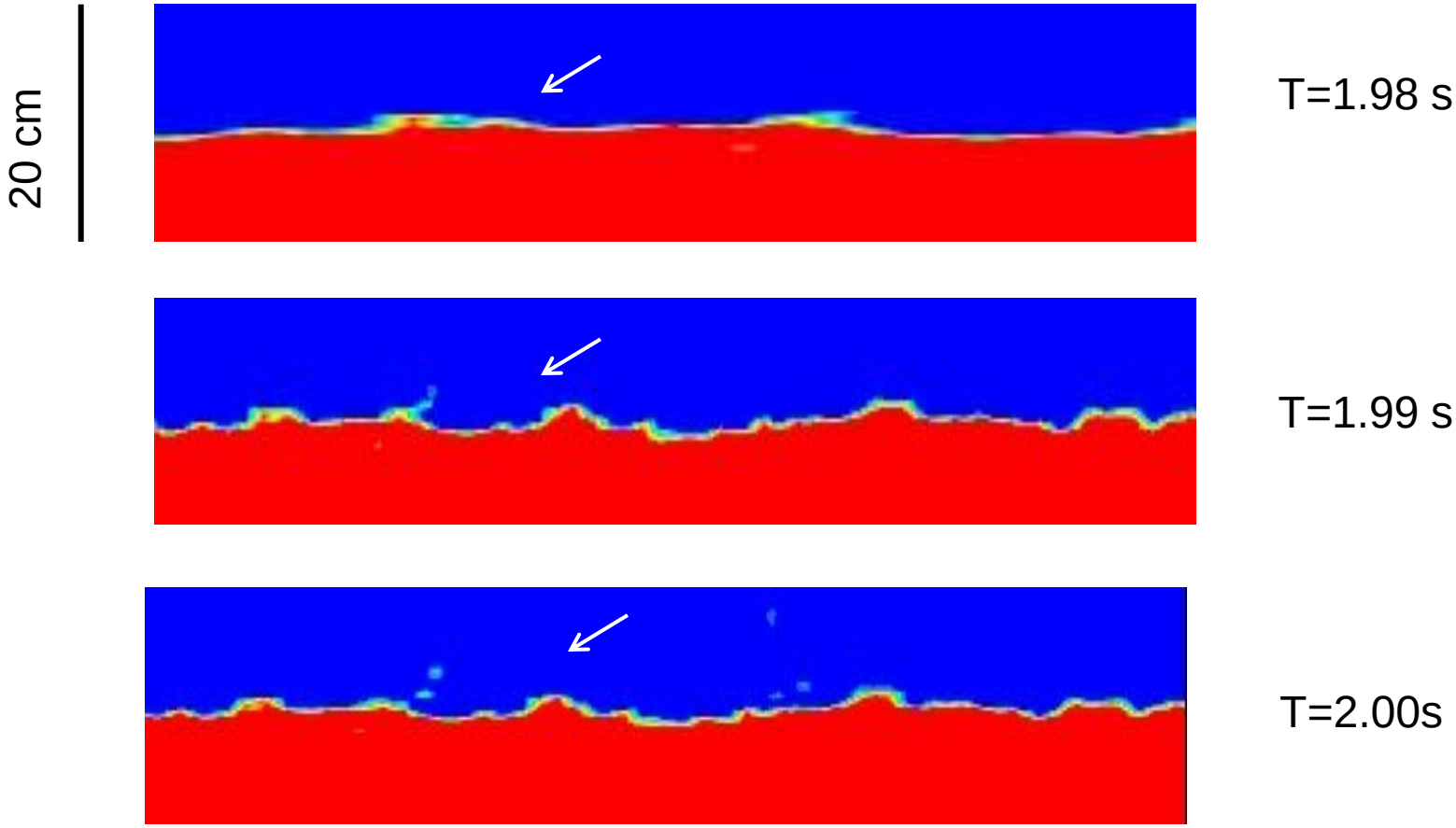

VOF-LES model

Large droplets produced by breakdown of small "projections"

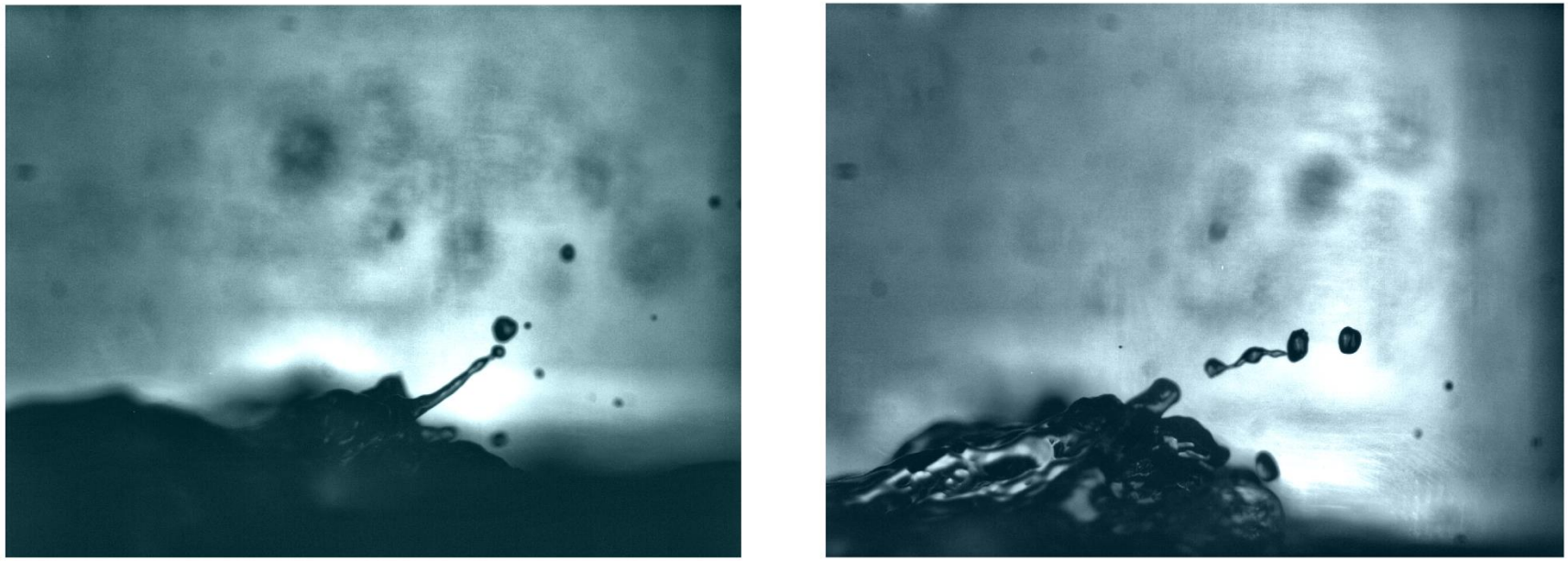

3 mm

Kelvin-Helmholtz instability may be considered as a suitable model for the creation mechanism of projections and spray in strong winds

Lab experiment at ASIST in collaboration with Brian Haus, Dave Ortiz-Suslow, Nathan Laxague

Streak-Like Structures on the Top of Wave Crests

Soloviev, Fujimura, and Matt (JGR, 2012)

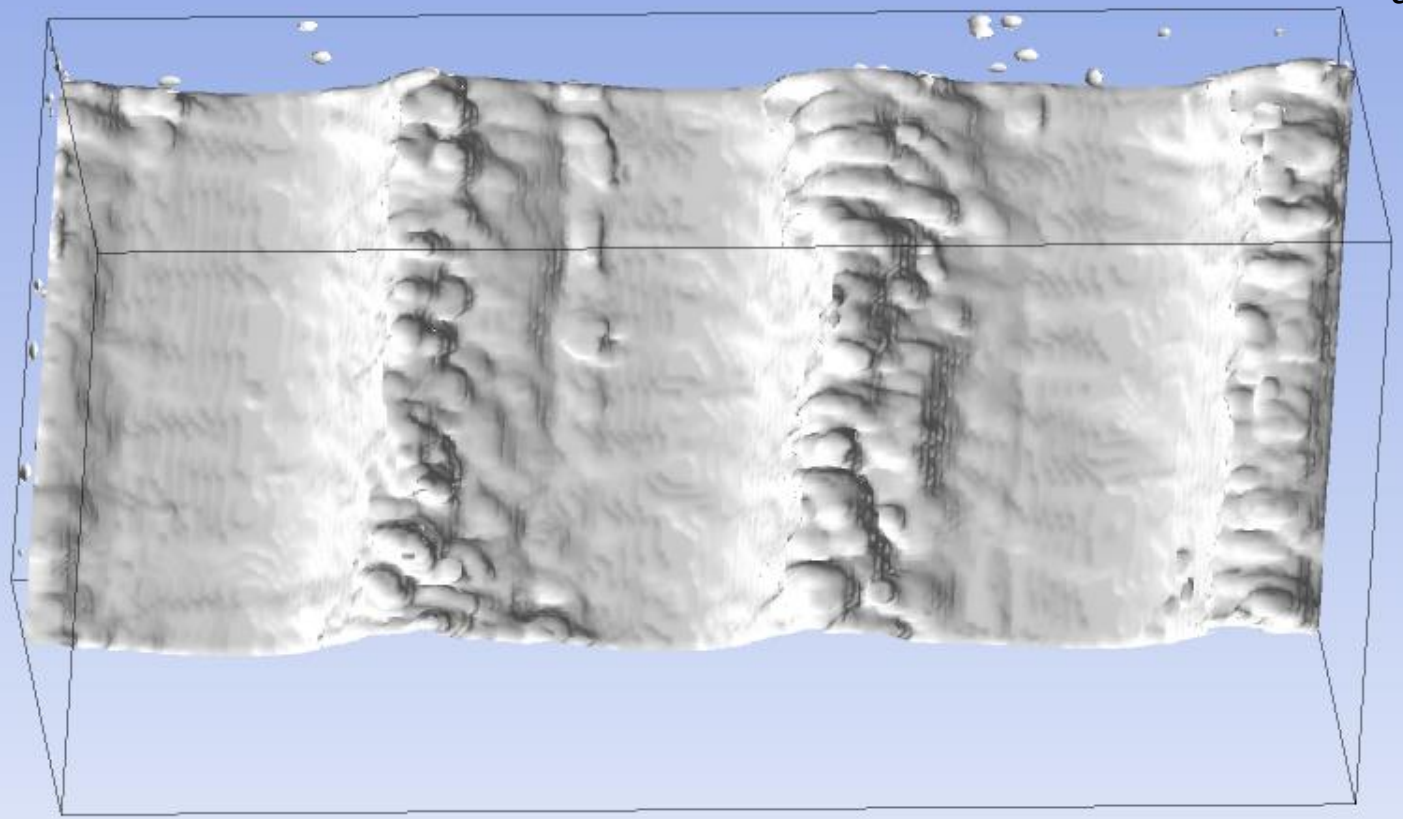

Spacing of streaks near a wall (Lesieur 2008): $d = 10\delta_\nu \sim 2$ cm

where : δ_ν - thickness of the viscous sublayer ($\delta_\nu = 11\nu / u_{*s}$)

u_{*s} - skin-friction velocity (a small fraction of the total friction velocity in hurricane conditions)

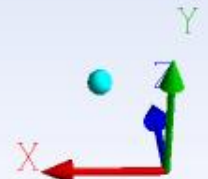

Foam streaks on the sea surface in hurricane conditions can be a result of KH instability at the air-sea Interface

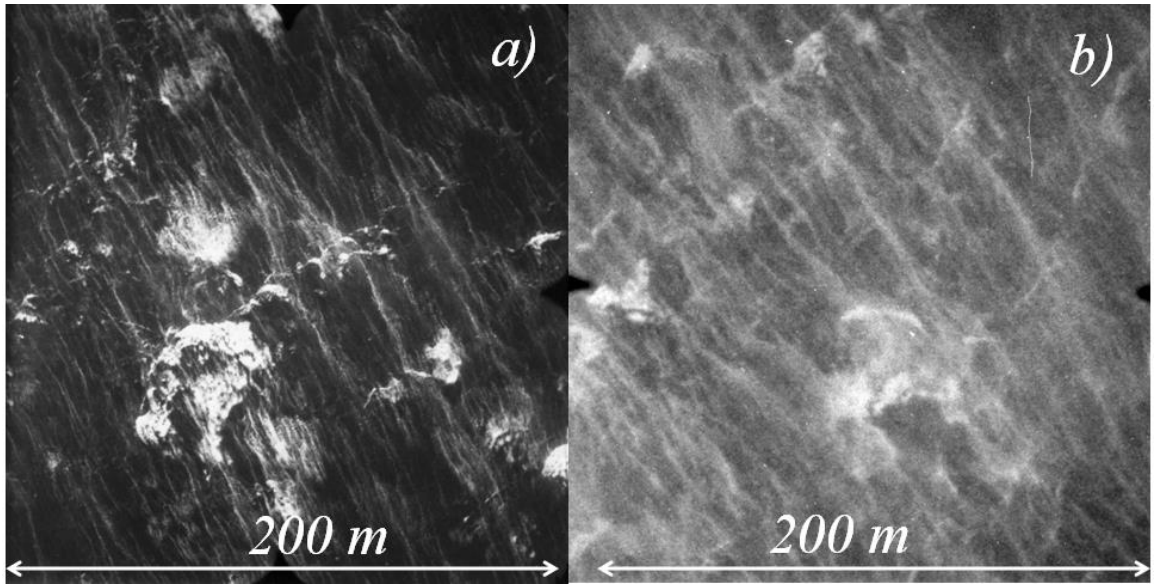

(a) Wind speed 28 m s^{-1}

(b) Wind speed 46 m s^{-1}

***Black et al.* (2006)**

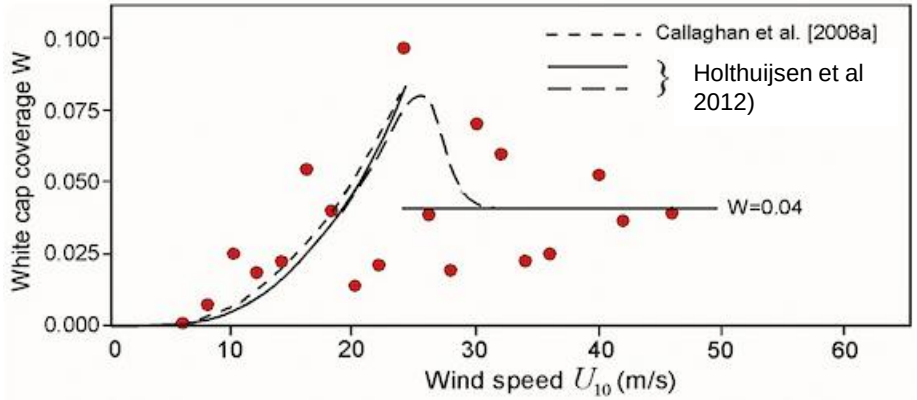

The white cap coverage increases with wind though at very high wind speeds remains at a constant 4% level, while the foam streak coverage increases toward full saturation (Holthuijsen et al. 2012).

Model Verification with Lab Data

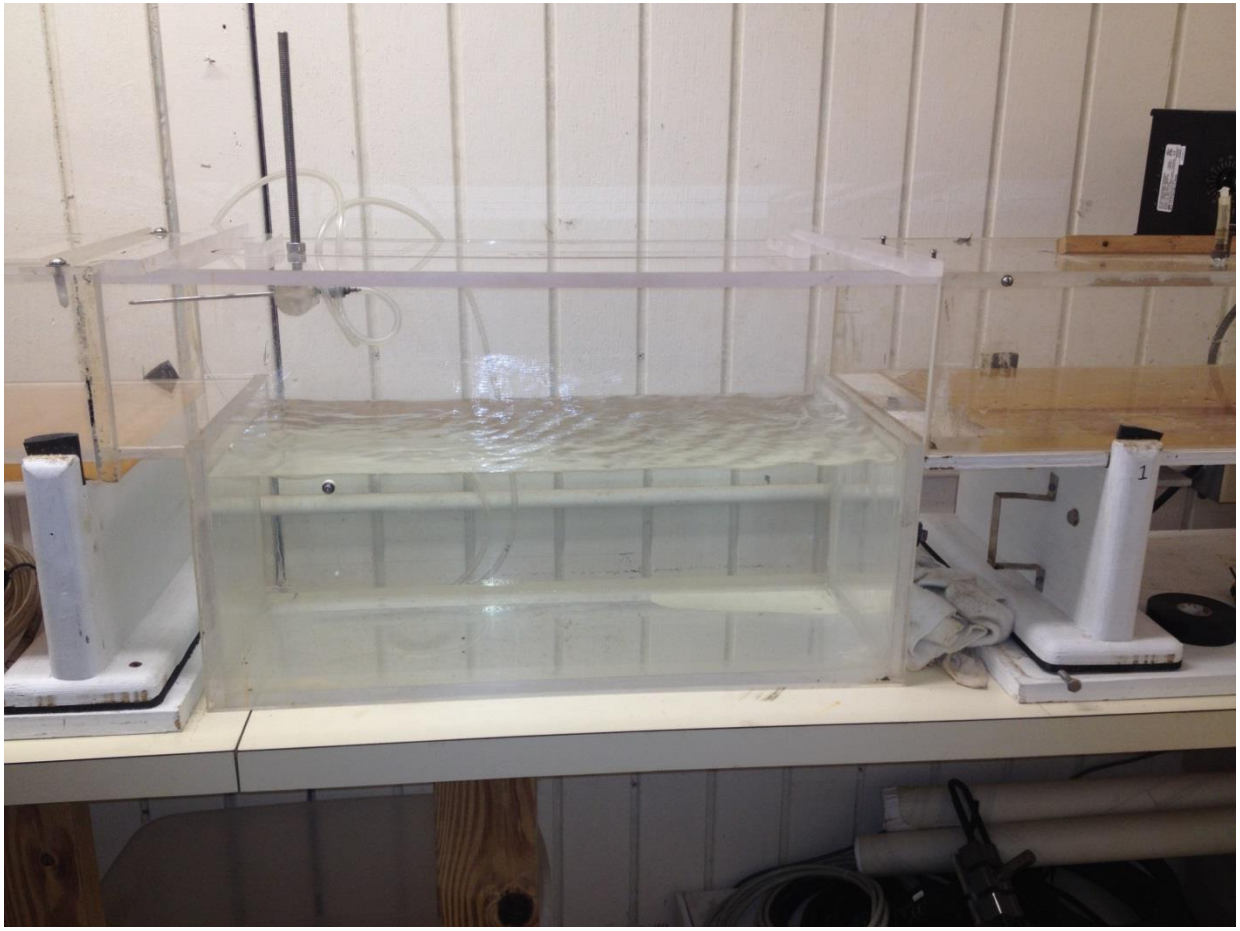

Lab experiment at UM RSMAS ASIST (in collaboration with Brian Haus, Dave Ortiz-Suslow, and Nathan Laxague)

Air-Water Interface: Numerical Simulation

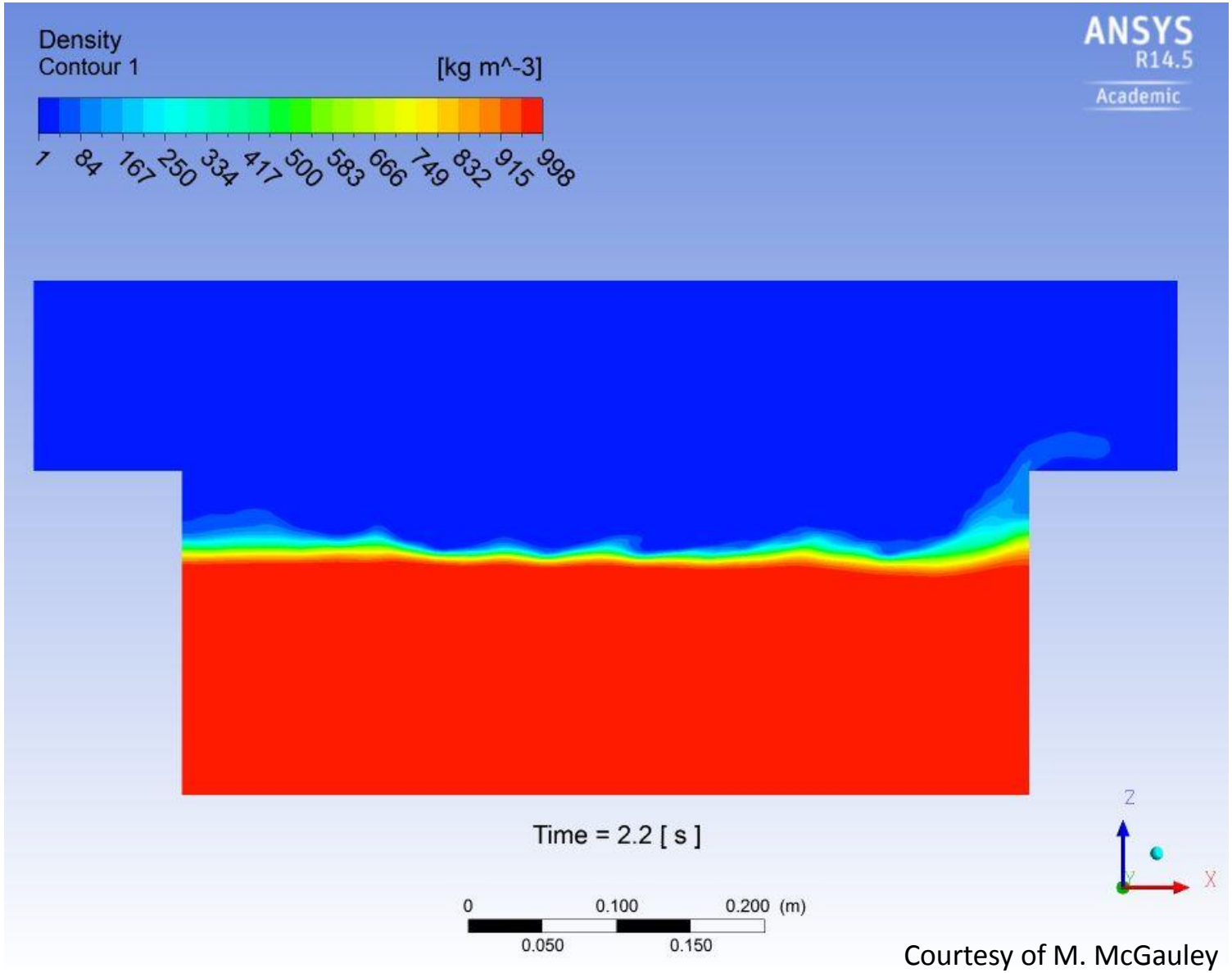

Courtesy of M. McGauley

Air-Oil Interface: Numerical Simulation

20 m/s

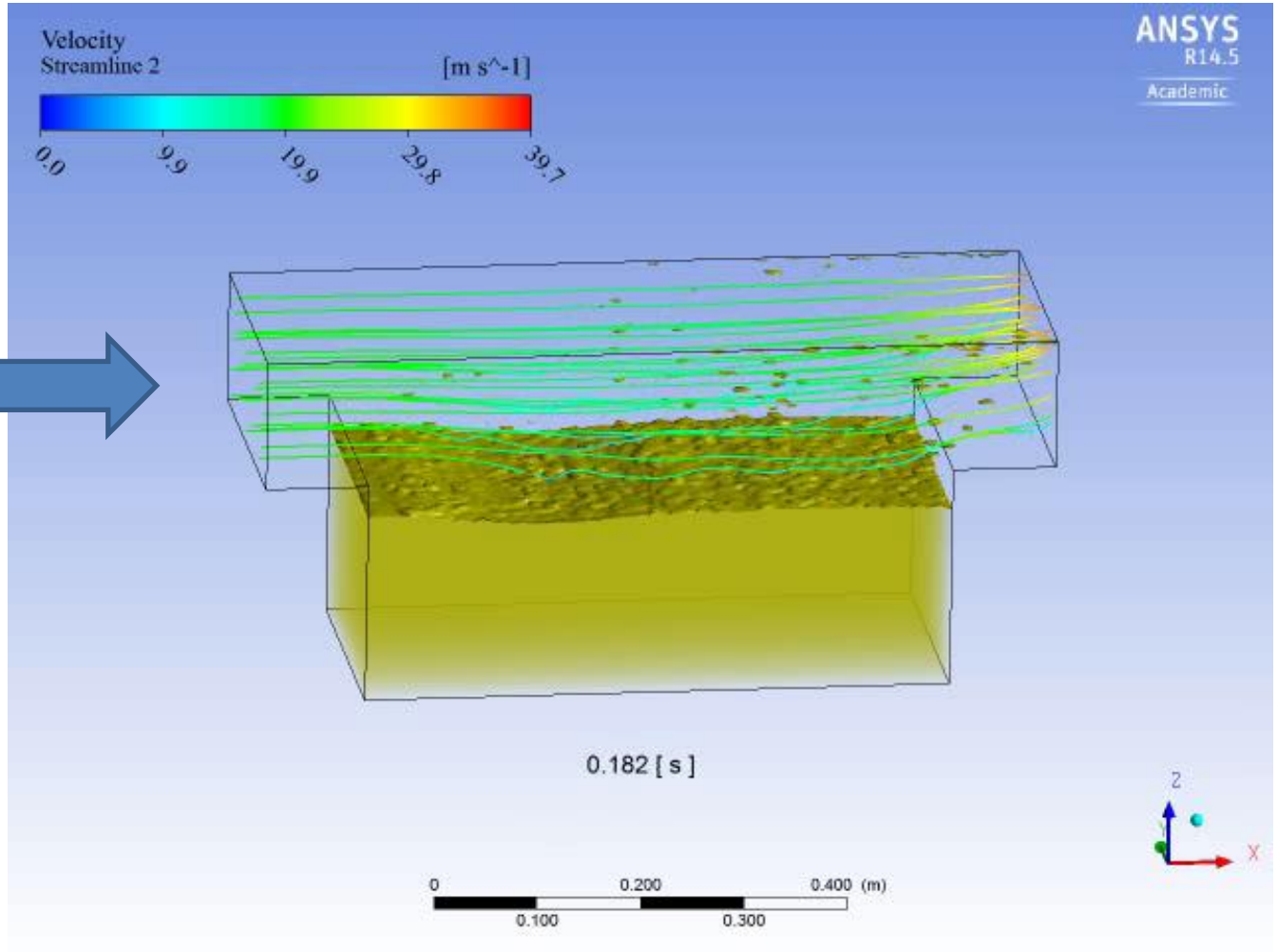

Courtesy of M. McGauley

Conclusions

- The variety of forcing factors, in combination with nonlinear feedbacks, result in a big variety of near-surface regimes
- Observations at the air-sea interface are a challenge and no universal tool exists
- Future progress is envisioned in combining theoretical, computational and laboratory results with available field data
- Parameterization of hydrocarbon fluxes at the air-sea interface is an important task in the problem of hydrocarbon transport and dispersion